CHAPTER

9

Characterizing Biopharmaceuticals using Analytical Ultracentrifugation

Steven A. Berkowitz[1], *John S. Philo*[2]

[1]Department of Protein Pharmaceutical Development, Biogen Idec, Inc., Cambridge, MA, USA

[2]Alliance Protein Laboratories, San Diego, CA

9.1 INTRODUCTION

Analytical ultracentrifugation (AUC) is a biophysical technique dating back to the early part of the twentieth century. In its initial development, it played a key role in demonstrating the existence of macromolecules via the pioneering studies carried out by Svedberg and his colleagues [1–7]. In the years following this ground-breaking work, the analytical ultracentrifuge was heavily used to characterize the macromolecular properties of biological and synthetic polymers. Although used in both areas, the analytical ultracentrifuge found its most effective application in the biological sciences where it has been employed to study the physical and chemical properties of proteins, nucleic acids, polysaccharides, and supramolecular structures (such as ribosomes, multisubunit enzymes, and viruses), which are unique to the biological world [8]. Of the several analytical ultracentrifuges that were commercially developed over these years, it was Beckman's Model E that was the work horse instrument employed to power the many experiments that drove the developments of molecular biology and biochemistry [2,9]. Probably one of the most notable contributions, other than the recognition of the existence of macromolecules (in particular the macromolecular nature of proteins) mentioned previously was the confirmation of the speculative ideas of Watson and Crick after their landmark 1953 paper [9] on the structure of DNA (which set the stage in the coming years for recombinant technology and the eventual development of the biopharmaceutical industry). This speculation concerned the mechanism by which DNA might conserve genetic information and pass this information on to future generations of offspring [10]. Meselson and Stahl, the scientists who conducted this famous AUC experiment [11], are frequently credited as having conducted "the most beautiful experiment in biology" [12].

In the biological sciences, the analytical ultracentrifuge was commonly used to (1) assess the solution molecular weight (MW) of biopolymers and the important molecular complexes that they formed; (2) assess the homogeneity and shape of these biomolecules and/or

Biophysical Characterization of Proteins in Developing Biopharmaceuticals
http://dx.doi.org/10.1016/B978-0-444-59573-7.00009-9

Copyright © 2015 Elsevier B.V. All rights reserved.

complexes; and (3) characterize their aggregation properties with themselves (self-association) and/or with other components (hetero-association). AUC analysis in these areas continued well into the 1970s until it was largely supplanted by other simpler, easier to use techniques such as size-exclusion chromatography (SEC) and sodium dodecyl sulfate-polyacrylamide gel electrophoresis (SDS-PAGE), particularly for the determination of MW and purity or sample homogeneity. In addition, at about this time interest in the biophysical chemistry of biopolymers started to wane and lose out to the growing developments in the fields of molecular biology and recombinant technology. Further developments in soft ionization techniques for inserting macromolecules into a mass spectrometer in the 1980s yielded much more accurate MW data, and further accelerated AUC's decline. As a result, usage of AUC and its further technical advances effectively disappeared except for a few, very small groups of individual scientists located in the US and in Europe. Given this situation Beckman effectively stopped supporting the instrument, and as a result maintaining the few existing operating centrifuges became a major challenge. However, as advances in molecular biology and biotechnology continued, the need to better understand the physical interactions of biopolymers, and especially proteins, began to return and so did interest in the use of AUC. Fortunately through the efforts of the handful of scientists still using the analytical ultracentrifuge, Beckman was convinced to develop a new instrument. This new analytical ultracentrifuge, the XL-A, incorporated many modern features, most notably automatic data acquisition, which took advantage of the explosive developments in personal digital computers and digital electronics [13–19]. This modernization of the analytical ultracentrifuge, coupled with the follow-on development of a series of new AUC data analysis software programs (by AUC users rather than by Beckman), opened the door for significant improvements in the capabilities of the analytical ultracentrifuge. As a result, AUC is today once again an important and capable technique in the arsenal of biophysical tools that is available to study biopolymers, including protein biopharmaceuticals [20–23].

9.2 UNIQUE FEATURES OF THE ANALYTICAL ULTRACENTRIFUGE THAT MAKE IT DIFFERENT FROM OTHER CENTRIFUGES

What makes the analytical ultracentrifuge different from other centrifuges commonly seen in a wide range of laboratories is its ability to allow the operator to actually watch and monitor quantitatively the migration of molecules of interest during the centrifugation process. Since this is done in a very well-controlled environment, accurate data can be acquired using UV [13], refractometric [24], and in some cases fluorescence detection [25]. At present there is only one commercial vendor, Beckman–Coulter, who makes the analytical ultracentrifuge (see Figure 9.1). A key element of the analytical ultracentrifuge is the analytical centrifuge cell (see Figure 9.2(H)), which consists of a centerpiece sandwiched between two separate optical windows. The centerpiece typically contains two openings or sectors to hold the analyte solutions (however it should be noted that other centerpieces exist for other special purposes, see Figure 9.2(A-G)). In using these centerpieces usually one sector will hold the reference buffer solution while the other sector will hold the sample solution (however, under certain conditions even the reference sector can contain a sample, which can effectively double the sample throughput per run [26]). An interesting point to note

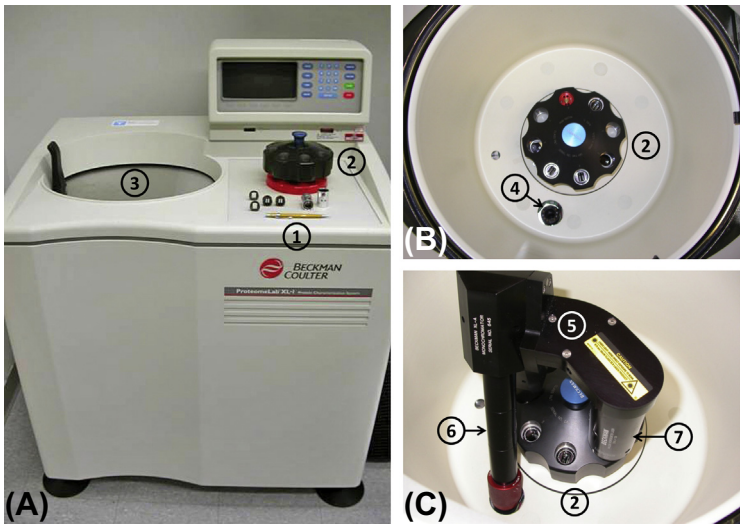

FIGURE 9.1 (A) Picture of the Beckman–Coulter XL-I analytical ultracentrifuge. Just above ① is an orange colored mechanical pen, which provides the reader with some perspective as to the size of the instrument, which is equivalent to a typical stand-alone high-speed preparative ultracentrifuge. Just above this pencil, to the right, are two assembled centrifuge cells (silver in color). Just to the left of ② is an 8-hole rotor. ③ is the armored door that opens to expose the centrifuge chamber. (B) With the centrifuge door open and looking straight down into centrifuge chamber. Just to the left of ②, at the base of the chamber is the 8-hole rotor that is sitting on the centrifuge's electric drive. The arrow for ④ is pointing to the opening at the base of the centrifuge chamber that allows the UV–VIS light to enter the chamber to eventually pass through the centrifuge cell. (C) Basically the same view as shown in "B" but with the optical bench, corresponding to ⑤, in place. Just above ② is again the 8-hole rotor, the arrow for ⑥ is pointing to optical bench for the incoming UV–VIS light that reflects the light down on to the rotor, while the arrow for ⑦ is pointing to the laser source for the Rayleigh interferometer. Note: the detectors for both the UV–VIS and Rayleigh interferometer are located at the base of the centrifuge chamber underneath the rotor.

is that the basic design, assembly, filling, and insertion of these cells into the centrifuge have changed remarkably little over the years since the start of the development of the analytical ultracentrifuge by Svedberg and his collaborators in the 1920's. [3].

9.3 THEORY

AUC experiments can actually be carried out in several different modes. However, these various modes can be segregated into two basic classes: (1) sedimentation velocity (SV, which we will refer to as SV-AUC in this chapter) and (2) sedimentation equilibrium (SE, which we will refer to as SE-AUC in this chapter). The key difference between these two classes of AUC experiments typically concerns the strength of the centrifugal field, which can easily be controlled by changing the rotation speed of the rotor. These two classes of AUC are also loosely associated with two classes of centrifuge centerpieces, which differ in both the shape and height of the solution column, as indicated in Figure 9.2.

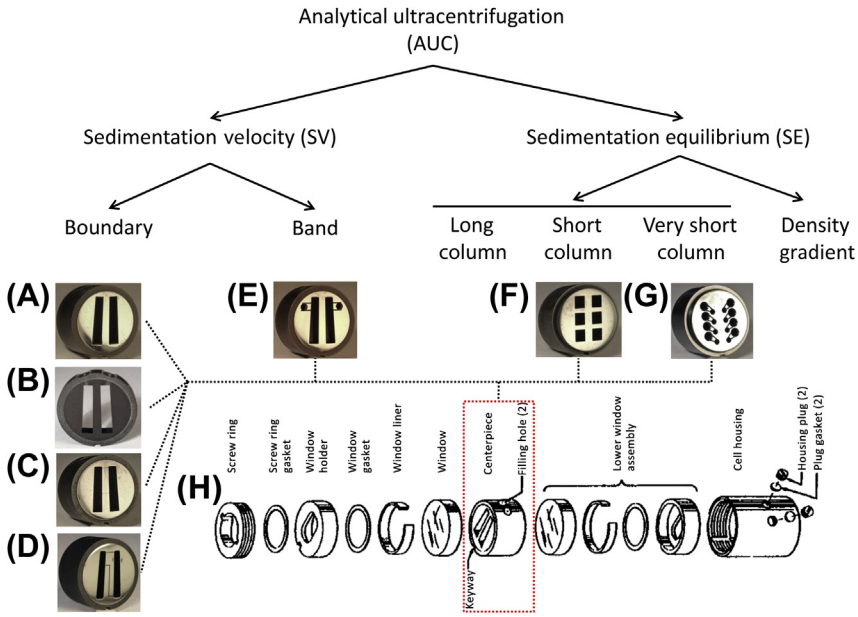

FIGURE 9.2 A diagram showing all the major forms of AUC along with the typical centerpieces (A–G) used to perform each particular form of AUC. SV-AUC can be divided into two sub-types, boundary and band SV-AUC. SE-AUC can be divided into one form that only varies in terms of the height (long, short, and very short) of the liquid sample column in the cell, and density-gradient SE-AUC, which requires the use of solution conditions that cause the sample to band at the buoyant density of the sample. Boundary SV-AUC centerpieces include the following: (A) standard 12-mm double sector, (B) 3-mm double sector (requires the use of the addition of two spacers for proper cell assembly), (C) 12-mm synthetic boundary (contains two thin channels connecting both sectors for the purpose of layering reference buffer on the sample to create a boundary and for matching the meniscus in both sectors when using interference optical detection), (D) a special 12-mm meniscus matching centerpiece (made by Spin Analytical, Berwick, Maine). Band SV-AUC centerpiece (E) 12-mm band-forming centerpiece. SE-AUC centerpieces include the following: (F) 12-mm 6-channel centerpiece that allows three samples (with their three corresponding buffer channels) to be run in one cell, (G) 12-mm 8-channel centerpiece that allows four samples (with their four corresponding buffer channels) to be run in one cell. (H) An exploded view of a typical 12-mm AUC cell that reveals all the typical parts required for its assembly. The component enclosed in red dots is the centerpiece that can correspond to any of the centerpieces (A–G) in this figure. Note: for long column SE-AUC and density-gradient SE-AUC centerpiece (A) is commonly used.

The strength of centrifugal field generated in any AUC experiment (the centrifugal acceleration) is equal to the product of the angular velocity, ω (expressed in radians/s), squared times the radial distance from the center of rotation, r (expressed in cm). As a result the strength of the centrifugal field in an AUC experiment is not a constant but rather increases linearly with radial distance, see Eqn (9.1).

$$\text{Centrifugal field} = \omega^2 r = [(\text{rpm})(2\pi)/60]^2 r \ \text{ expressed in units of cm/s}^2 \tag{9.1}$$

In the case of classical boundary SV-AUC, which is by far the most common form of AUC conducted today in the biopharmaceutical industry, the centrifugal field has sufficient strength to cause the protein molecules of interest to migrate from the meniscus

to the bottom (or base) of the AUC cell, usually over a timescale of several hours or longer. This migration of the protein molecules as a function of time is of key importance in these experiments and is characterized by an experimental molecular parameter called the sedimentation coefficient, s. The value of s for a given protein is a parameter that is specific to a particular protein-formulation combination and experimental conditions used in an AUC experiment. Experimentally s is simply defined as the ratio of the velocity with which a protein molecule moves in the centrifugal field to the field strength, as shown by Eqn (9.2):

$$\begin{aligned}\text{Sedimentation coefficient} = s = \text{velocity/centrifugal field} &= v/\left[\omega^2 r\right] \\ &= [\mathrm{d}r/\mathrm{d}t]/\left[\omega^2 r\right] = [\mathrm{d}\ \ln(r)/\mathrm{d}t]/\left[\omega^2\right]\end{aligned} \tag{9.2}$$

From Eqn (9.2) it can be seen that s is expressed in unit of seconds. It turns out the sedimentation coefficients of many important biological molecules and substances fall in the range from roughly 10^{-13} to 10^{-11} s. Therefore, for convenience, and also to honor Theodor (The') Svedberg, values of s are usually reported in Svedberg units (using the symbol S), where $1\ \mathrm{S} \equiv 10^{-13}$ s. Hence a protein molecule with a sedimentation coefficient value of 5.3 S actually equals 5.3×10^{-13} s.

The velocity a protein molecule reaches in an SV-AUC experiment, which is characterized by that molecule's sedimentation coefficient, turns out to be determined by the summation of three forces (F), that we will see are influenced by the physical and chemical properties of a protein in its formulation buffer in combination with the centrifugal field (as defined in Eqn (9.1)). These three forces include:

1. *The centrifugal force* (F_c) that drives molecules to the base of the AUC cell, which is equal to the product of the centrifugal acceleration ($\omega^2 r$) times the mass of the molecule. If M is the molar mass of the protein, dividing it by Avogadro's number (N_a) yields the mass of one protein molecule, and hence we get $F_c = (M/N_a)\omega^2 r$.
2. *The buoyant force* (F_b) that opposes F_c, which according to Archimedes principle is equal to the weight of the solvent displaced by an object placed into a solution. In the case of an AUC experiment, the weight is not from the earth's gravitational field, but rather the weight generated by the centrifugal field ($\omega^2 r$). Hence, if M_0 is the mass of the solvent displaced by a macromolecule, then $F_b = -M_0(\omega^2 r)$. M_0 is related to the partial specific volume, $\overline{v}_2$, of the sedimenting protein (or other molecule), which is defined as the change in solution volume (in mL) on dissolving 1 g of protein. Hence in an AUC experiment M_0 is then simply equal to the mass of one protein molecule, (M/N_a), times $\overline{v}_2$, (which is the volume of liquid displaced by that one protein molecule) times the buffer solution density, ρ_0. Hence, $M_0 = (M/N_a)(\overline{v}_2\rho_0)$, is the mass of the buffer solution displaced by the one protein molecule when placed into the formulation buffer.
3. *The frictional force* $(F_f) = -fv$, also opposes F_c, where f is the frictional coefficient of the protein molecule which characterizes the hydrodynamic friction of the molecule as it moves through a solution under a driving force. This frictional coefficient depends on the overall size and shape of the molecule.

Upon placing a protein molecule in a centrifugal field the molecule will quickly (within nanoseconds) [27] reach a constant velocity. At this point the sum of these three forces will equal zero:

$$F_c + F_b - F_f = 0 = \left[\left(M/N_a\right)\omega^2 r\right] + \left[(M/N_a)(v_2\rho_0)\left(\omega^2 r\right)\right] - [fs\omega^2 r] \tag{9.3}$$

On rearranging this equation, using Eqn (9.2), and after noting the fact that the translational diffusion coefficient, D, of the molecule is given by $kT/f = RT/N_a f$ (where k equals the Boltzmann constant), one obtains Eqn (9.4), the famous Svedberg equation:

$$s = [M(1 - \overline{v}_2\rho_0)]/[N_a f] = [M(1 - \overline{v}_2\rho_0)D]/[RT] \tag{9.4}$$

Note that in Eqn (9.4), the quantity $M(1 - \overline{v}_2\rho_0)$, is defined as the "buoyant mass" of the protein molecule (its molar mass less the mass of the buffer solution it displaces). This key quantity provides the driving force for sedimentation, and therefore is the experimental parameter directly measured in AUC experiments.

From these simple equations it can be seen that these three forces acting on the sedimenting molecule depend on several factors that are unique properties of the protein being studied. Those factors include (1) the protein's buoyant mass (which depends on its amino acid composition, glycosylation, and the density of the formulation buffer) (2) its frictional properties, which depend on its overall size and shape (conformation or three-dimensional structure), (3) its hydration (the amount of water bound on its surface) and (4) solvation or preferential solvation effects (exclusion of excipients, or binding of excipients at the protein surface). All of those properties may vary depending on the formulation buffer composition and/or the temperature. As a result, determining the sedimentation coefficient of a protein drug is a very useful parameter for characterizing these drug molecules and for assessing the biophysical comparability of their higher-order structure (HOS) and their physicochemical properties.

In subsequent sections of this chapter we will discuss how these simple physical attributes of a protein play an important role in SV-AUC and SE-AUC experiments in allowing useful information about the biophysical properties of these protein drugs to be obtained. However, before moving on, some interesting consequences of Eqn (9.4) as well as a comment about the oversimplifications of the physical picture used in developing Eqn (9.4) should be noted in order for the reader to get a more accurate understanding about AUC and its utility in the biopharmaceutical industry:

- The impact of chemical heterogeneity and solution density in characterizing protein drugs

  Noting the buoyancy term $(1 - \overline{v}_2\rho_0)$ in Eqn (9.4), given the typical protein value for $\overline{v}_2$ of about 0.73 mL/g, and given that buffer solution densities for protein drugs are usually close to that of water ($\rho_0 \cong 1.0$ g/mL), in AUC experiments one would expect proteins to sediment to the bottom of AUC cell. This is also true for glycoproteins (protein molecules with covalently bond carbohydrates attached to them). Since carbohydrates are even denser than polypeptides, having $\overline{v}_2$ values close to 0.6 mL/g [28], the v_2 values for glycoproteins would typically be even lower than 0.73 (how much lower will of course depend on the amount of carbohydrate that is attached to the protein). However, for lipoproteins (protein molecules with covalently or noncovalently bound lipids), and for

membrane proteins solubilized in detergents (yielding proteins with noncovalently bound detergent), their values for $\overline{v}_2$ can be significantly greater than 0.73. In fact when the ratio of lipid or detergent to protein is high enough, a lipoprotein or detergent-solubilized membrane protein can have a value for $\overline{v}_2\rho_0$ that is actually greater than 1, yielding a negative buoyant mass and causing these type of protein molecules to actually float (migrate form the cell base toward the center of the rotor) during AUC instead of migrating to the bottom of the centrifuge cell.

- Hydration and preferential interactions

  In generating Eqn (9.4), two simplifications were made that can have significant impact that the reader should be aware of. These assumptions include (1) that the water of hydration of the protein (the water that is bound and moves with the protein during AUC) has the same bulk properties as water that is free in the bulk solution (that is, the density or partial specific volume of the bound and unbound water is the same) and (2) the AUC experiment was carried out in a two-component solution (water, 1, and protein, 2). Unfortunately the latter situation is virtually never the case (and actually should not be true since pure water at zero ionic strength is really not an appropriate solvent for AUC on charged macromolecules). Biopharmaceutical solutions contain excipients, the most important of which is a buffer to maintain the solution pH. In addition, other excipients (salts, nonionic detergents, sucrose, etc.) are usually added for various reasons, the most common of which is the need to maintain long-term chemical and physical stability of the protein drug. As a result, protein drug solutions are actually multicomponent solutions. The ramifications of this require a more rigorous formulation of Eqn (9.4), which is beyond the scope of this chapter. However, if the buoyancy term $(1 - \overline{v}_2\rho_0)$ is replaced by a term called the protein's density increment [29–31] the complicating effects of hydration and preferential interactions can be accounted for to yield accurate protein molar mass values. A protein's density increment can be experimentally assessed via a series of protein solution density measurements at different protein concentrations, where all protein solutions are dialyzed against the same formulation buffer until chemical equilibrium is reached (also referred to as constant chemical potential). Note however that experimental values of partial specific volumes or density increments are not needed for most of the common applications of AUC in the biopharmaceutical industry.

9.4 UTILITY OF AUC IN THE BIOPHARMACEUTICAL INDUSTRY

Today for biopharmaceutical characterization, and particularly for process development area, the analytical ultracentrifuge can play an important role in the following key areas:

1. To assess and characterize the aggregation present in biopharmaceuticals via a method that is independent of (or orthogonal to) SEC. The utility of AUC in this area is of particular importance given the high level of concern about aggregation for these drugs, and SV-AUC is the primary technique used for this purpose. Although SEC is the work horse analytical tool used in the industry to assess aggregation, making sure

an SEC method is providing valid aggregation information is not that straightforward (see Chapter 7 in this book on SEC). Hence because AUC can provide independent information about the amounts and size distribution of the aggregates in a biopharmaceutical sample in its formulation buffer, with virtually no method development, using different physical principles than SEC, and because it is immune to a number of the issues that can adversely affect SEC results, AUC serves two very useful purposes: (1) providing a reasonably quick and fairly reliable estimate of the level of aggregation that is present in a sample during the earlier stages in the development of a new protein drug, until a functioning SEC method is put into place; and (2) giving a level of assurance that the SEC method being used is in fact providing meaningful aggregation information even if the formulation buffer of the sample and the SEC mobile phase differ. This latter point is usually assessed by demonstrating that the total amount and distribution of aggregates for the same sample by both techniques is in reasonable agreement. However, the issue here is what constitutes reasonably good agreement? One criterion is that the SEC protocol should not fail to detect (or grossly underestimate) aggregate species which are routinely detected by SV-AUC. With respect to the total aggregate content of the samples, agreement between SEC and SV-AUC to within about ±2% is not unreasonable. This level of disagreement might seem to some to be too large to be really considered "in agreement" or "useful". However, if one considers the general limit of quantitation (LOQ) for determining aggregate content of a sample by both methods, one will realize that this ±2% is not that unreasonable. In the case of a well-functioning SEC method a typical LOQ falls in the range of 0.1−0.5% [23,32], while in the case of SV-AUC the typical LOQ falls in the range of 1−3% [33−38]. The almost order of magnitude difference in LOQ between these two methods clearly complicates things, forcing us to use the least accurate method as a guide to establish what defines "in agreement". This topic will be discussed in more detail later in Section 9.5.6.1.

AUC is a far more versatile method than SEC for characterizing the heterogeneity of a protein drug and its aggregates. This versatility arises from the uniquely large size range of molecules that can be characterized by AUC by simply varying the rotor's speed. For proteins and peptides the molar mass range of AUC is approximately from a few hundred to 10^9 Da. That range far exceeds the typical capability of analytical SEC, especially in terms of any one type of SEC column. Hence biopharmaceuticals ranging from small peptides to very large protein biopharmaceutical particles such as viruses, virus-like particles (VLPs), or nanoparticles used in vaccines and drug delivery systems, can all be easily characterized using AUC.

2. As a general tool to characterize the HOS or conformation of protein drugs and for assessing the comparability of the HOS between different samples of the same protein drug by determining the sedimentation coefficient of the monomer species in these samples[1]. Like spectroscopic methods such as circular dichroism (CD) or intrinsic fluorescence, the information derived from the sedimentation coefficient reflects a collection of global properties of the protein molecule, which include MW, shape,

[1]In this context by "monomer" we really mean whatever is the normal oligomeric state of the biomolecule (the main peak).

solvation properties, microheterogeneity in terms of posttranslational modifications (PTMs), and normal fluctuations in conformation (as discussed in Chapter 1 of this book). This global property of the sedimentation coefficient would normally make it rather insensitive to small changes in any one of these properties. However the uncertainty to which this parameter can be measured on a routine basis is typically less than ±1% at a confidence limit approaching 95% (and even less for comparisons when all samples are present in the same AUC run). Furthermore, the sedimentation coefficient can change a factor of two- to three-fold when a native protein unfolds, which is a larger change than that observed for spectroscopic techniques commonly used for demonstrating comparability of HOS such as CD and intrinsic fluorescence. Hence the high precision to which sedimentation coefficients can be measured, along with the large range of values that this parameter can span for a monomeric protein, can to some extent offset its generally low spatial resolution for detecting small differences in the HOS of different samples of the same molecule. In fact there are special difference modes for carrying out SV-AUC that enable extremely small changes in the sedimentation properties of protein drugs to be detected with very high precision [39,40], see Section 9.9.2.2. As a result, measuring the monomer sedimentation coefficient of samples of the same protein drug obtained from different manufactured lots or made using different production procedures or even by different companies (e.g., biosimilars) represents an excellent choice for assessing biophysical comparability between samples in terms of their HOS.

3. For generating quantitative and/or qualitative (visual) information to detect and characterize the self-association properties in protein drugs, potentially even at high concentrations approaching 40–50 mg/mL via SV-AUC and possibly much higher concentrations (20–200 mg/mL) using SE-AUC (see section 9.7.2).

9.5 BOUNDARY SV-AUC

Today in the biopharmaceutical industry, especially in the process development area, by far the most common form of AUC conducted is SV-AUC in the form of boundary SV-AUC. The primary reasons for this are the high information content of this mode, as well as the typically much shorter time required to conduct these experiments relative to SE-AUC. In addition, the important development of powerful computer software analysis programs over the last 2+ decades has enabled the higher resolution and higher sensitivity capabilities of SV-AUC to be realized. Hence most of this chapter on AUC will focus on SV-AUC Nevertheless toward the end of this chapter we will also discuss the other major form of AUC, SE-AUC, which is still a useful and capable tool, particularly in combination with SV-AUC.

9.5.1 Boundary SV-AUC on a Homogeneous Protein Sample—Measuring a Protein's Sedimentation Coefficient in the Absence of Diffusion (in the Theoretical World)

In conducting a boundary SV-AUC experiment on a homogeneous protein the resulting data output consists of a series of data scans, which typically are separated by a constant time interval over the course of the SV-AUC run. Each data scan, $c(r,t)$, consists of a

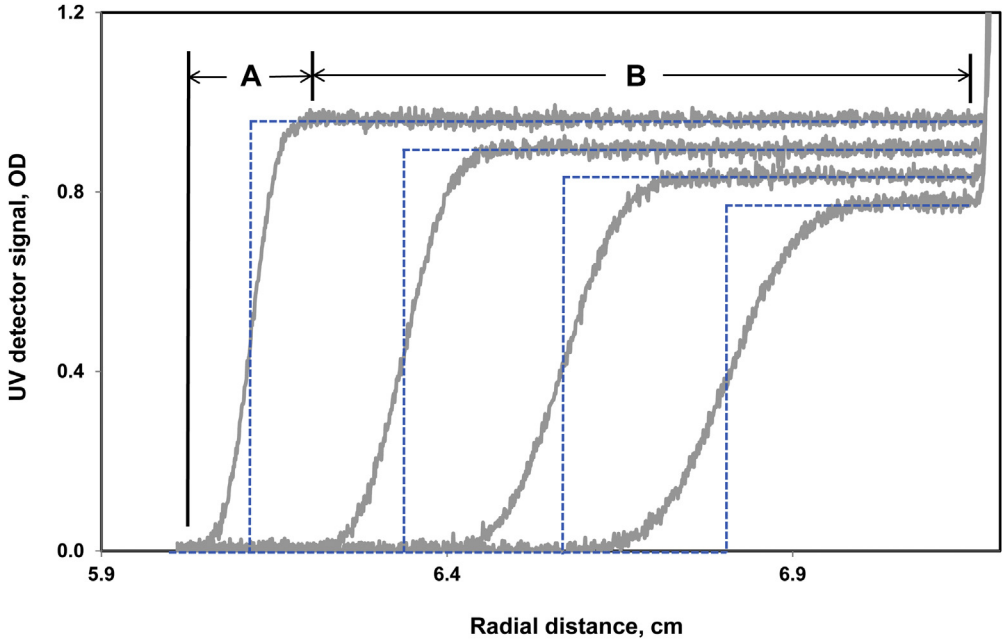

FIGURE 9.3 Four detector scans (gray traces) from a simulated boundary SV-AUC experiment using SEDFIT on a dilute homogeneous 150 kDa protein solution at 40,000 rpm taken at different times during the experiment. Part "A" region of the first data scan shows the corresponding "boundary region" of the scan, while part "B" of the same scan corresponds to the "plateau region" of the scan. The blue dashed profiles are the same corresponding data scans but without sample diffusion and noise.

detector signal readout, e.g., UV absorbance reading, of the protein sample in an AUC cell during centrifugation as a function of radial distance from the center of rotation, r, at a given time, t. In the absence of diffusion the migration of a homogeneous protein in the centrifugal field would yield data scans with an infinitely sharp *boundary* and a flat *plateau* that decreases with time due to the radial dilution effect arising from the sector-shaped compartments of a centrifuge cell that holds the sample (as shown in Figure 9.3 by the blue dashed profiles). This sector shape is actually required, and is a critical element of any successful SV-AUC experiment. This need for a sector shape cell arises due to the radial nature of the centrifugal field and molecular flow. It is essential that the flow remains parallel to the walls of the sector. Any deviation from the appropriate sector shape and its appropriate alignment within the centrifugal field could lead to the flow hitting the walls, producing a local concentration increase that could violate the necessary stability criteria of a nonnegative density gradient across the entire sample solution running from the meniscus to the base of the solution compartment. If a negative density gradient is encountered anywhere along this path, solution inversion (mixing) will occur as a result of the density difference, leading to convective transport of the protein molecules causing erroneous sedimentation data to be generated. The potential occurrence of such a problem is of most concern for very dilute protein solutions (e.g.,

a few tens of μg or less/mL) that also contain very low levels of salt, buffer, or other excipient components (e.g., a few mM or less). These conditions can also make the solution more prone to thermal nonhomogeneity (gradient) effects that can also cause convective mixing. In most cases, however, the tens of mM level of salts and/or buffer and other excipient components present in solution, in combination with the high centrifugal field, will generate a sufficient density gradient to stabilize the sample solution to prevent convection for the 1 mg/mL or lower protein concentrations commonly used in SV-AUC experiments. At the same time, however, the resulting density gradient and corresponding viscosity gradient that is generated by the excipients is generally too small to have a significant impact on the migrating properties of the protein molecules. Nevertheless, in the presence of high excipient concentrations in high centrifugal fields situations can arise where the resulting density gradient and (more important) viscosity gradient actually do need to be accounted for during data analysis [40] to achieve the high analytical accuracy and sensitivity to minor components [41] normally attained with SV-AUC.

It can be seen from Eqn (9.2) that plotting ln(r) versus time, t, where r corresponds to the radial position of the infinitely sharp boundary, will yield for a homogeneous protein a straight line (in the absence of any concentration-dependent effect that could alter the migration of the protein molecule), whose slope is directly proportional to the sedimentation coefficient of the homogeneous protein.

9.5.2 Boundary SV-AUC on a Homogeneous Protein Sample—Measuring a Protein's Sedimentation Coefficient in the Presence of Diffusion (in the Real World)

In the real world, molecules diffuse. Given the temperatures used and the time required for protein samples to sediment the approximate 1.2 cm from the meniscus to the bottom of a centrifuge cell, significant broadening of the migrating sedimentation boundary is normally encountered during SV-AUC experiments. Hence for a homogeneous protein sample each data scan in an SV-AUC experiment will not yield an infinitely sharp boundary, but rather a single sigmoidal shape boundary, as shown in Figure 9.3, due to the radial diffusion of molecules both toward and away from the center of rotation. It should also be realized that this broadening is further compounded by the radial variation of the centrifugal field, since as protein molecules diffuse away from and toward the center of rotation they will migrate into stronger and weaker centrifugal fields respectively (see Eqn (9.1)), which will further enhance the diffusional broadening of the migrating boundary. While diffusional broadening fundamentally limits the resolution of different species, on the other hand it is this diffusional broadening which provides the information about the molar mass and shape of each sedimenting species in a velocity experiment (because M, s, and D are interrelated through the Svedberg equation, Eqn (9.4)).

Hence with the presence of diffusion a question now arises as to what position in the migrating boundary does one use to follow the migration of the protein boundary to assess its sedimentation coefficient? Years ago it was very common to just use the radial position corresponding to the half-height of the plateau or to use the position of the peak maximum in a derivative plot of each scan (which was directly provided years ago using the Schlieren optical system on the old analytical ultracentrifuges). However, Goldberg showed in 1953

[42] that the correct radial position to use for each scan corresponds to the square root of the second moment of the sedimenting boundary, r_{srsm}. However, for highly homogeneous samples using the half-height of the plateau, instead of r_{srsm}, had a negligible impact on the calculated s value. Today this approach of plotting the natural logarithm of the appropriate radial boundary position with respect to time for assessing s is no longer used.

In sections 9.5.4 and 9.5.5 we will discuss how the above simple mode of AUC data analysis has now been replaced by modern modes of SV-AUC analysis that can yield various levels of information about the level of homogeneity or conversely the level of heterogeneity and physicochemical properties of a protein drug.

9.5.3 Assessing the Homogeneity of Protein Biopharmaceuticals: the Influence of Various Forms of Sample Heterogeneity on Boundary SV-AUC Data

In general, as a protein biopharmaceutical reaches its terminal stages of purification, it should correspond to highly purified material consisting of only one protein. Heterogeneity from the presence of other proteins (e.g., host cell proteins), other biological macromolecules (e.g., nucleic acids or polysaccharides), and viruses should be far too low to be detected by AUC analysis at the drug substance (DS) and drug product (DP) stage. Unfortunately, there are several factors that conspire to introduce various forms of heterogeneity into protein drugs. One of the most basic factors common to all proteins is the intrinsic dynamic variability of protein folding that gives rise to an ensemble of native structures or conformations that a protein drug will populate at any time, and which varies from one protein to another and with solution and environmental or experimental conditions (as discussed in Chapter 1 of this book). Nevertheless, the nature of this ensemble of conformations should be a unique characteristic of the drug protein and its physicochemical environment, and should correspond to a single time-averaged sedimentation coefficient. Changes in this ensemble of conformations can occur via exposure to physical stresses that can lead to nonchemical modifications, which alter the range of conformations available to the protein drug, or the time spent in a given conformation, as a result of changes in some of its weak noncovalent interactions (again see discussions in Chapter 1 of this book). Such changes could be reflected in changes in the sedimentation coefficient and the shape of the sedimentation boundary of the native form of the protein drug. Under rather extreme cases this could even give rise to the appearance of an additional resolved boundary or boundaries moving faster or slower than the normal main boundary (depending on the extent of the change in conformation, its lifetime, the fraction of material present in these different forms, and the signal to noise ratio (S/N) of the data collected). Such changes can also alter the self-association (aggregation) properties of the molecule, leading to changes in oligomerization that will also alter the sedimentation boundaries.

A second factor that can impact the level of heterogeneity associated with a protein drug concerns the type and level of covalent chemical modifications present on these drug molecules, called post-translational modifications (PTMs), arising in vivo during its synthesis and folding within the cell or in vitro during purification, vialing, filling, and storage. Such PTMs also include cleavage of peptide bonds, producing either nicks (where fragments that are formed remain noncovalently associated, but perhaps resulting in increased flexibility in the protein drug) or actual fragmentation of the intact protein drug (dissociation of the

clipped fragments). These forms of heterogeneity are often referred to as microheterogeneity because they are commonly present at only low levels and more importantly due to the high similarity of their HOS to the normal form of the molecule. These chemical modifications can, like the physical modifications mentioned above, lead to changes in the sedimentation coefficients and/or self-association of the protein drug that in turn impact the sedimentation data in the same way.

A third factor contributing to a protein drug's heterogeneity is the presence of noncovalent and/or covalent aggregates. These aggregates could be specific to the main or variant forms of monomeric protein drug, or to a combination of both. The presence of such aggregates in the final protein DS or DP could be due to a combination of reasons. One can be the ineffectiveness of the purification process in removing aggregates that formed at any time prior to the last purification step capable of removing them, e.g., during cell culture production. A second may be the induction of aggregates any time after the last purification process step that is capable of removing them, e.g., filling, vialing, or during long-term storage.

What is typically unique about aggregation heterogeneity is that the accompanying large increase in mass usually gives rise to some very noticeable (visual) features in the recorded SV-AUC data scans. These features include unique, resolved, faster-moving boundaries or significant asymmetry of the monomer boundary, with upwardly sloping plateau ahead of the main boundary due to the usual significantly higher sedimentation coefficient of this aggregated material. Unfortunately the ability to visually observe such features in the SV-AUC data scans depends on the sharpness of the migrating boundary and the amount of the aggregated material present relative to the signal to noise (S/N) of the data (see Figure 9.4), with the former being highly dependent on the MW of the material analyzed. It should also be noted that since sedimentation coefficients are a function of both mass and shape of the migrating material (see Eqn (9.4)), changes in shape that cause increasing frictional effects (drag) can potentially offset the higher mass of the aggregate, leading to some surprising SV-AUC results, e.g., larger MW (but partially unfolded) aggregates migrating slower than smaller MW aggregates which are more compact.

A fourth factor that can contribute to the heterogeneity of a protein drug concerns the potential for reversible concentration-dependent physical interactions between the native monomer, variant forms of the monomer, or complexes of the normal monomer and variant forms, to yield aggregated material. Proteins displaying such properties in solution are commonly referred to as self-associating or chemical-reacting systems. The presence of such physicochemical behavior in a protein drug will significantly influence SV-AUC experiments as mentioned in the case for stable aggregates. However the influence of these self-associating protein systems can be much more complex than for the stable aggregates, depending on the strength of the association, the kinetics of the association−dissociation reactions, and the shape of the actual aggregate(s) formed [43−46].

Unfortunately one or more of these forms of heterogeneity can be (and usually is) present in any protein biopharmaceutical. In addition, each of these forms of heterogeneity could themselves be generated by more than one route, process step, or mechanism. Hence the resulting sedimentation data can be complex, resulting in a unique biophysical signature (or fingerprint) of the drug and its physicochemical properties. A key goal of the biophysical scientist in the biopharmaceutical industry is the characterization and

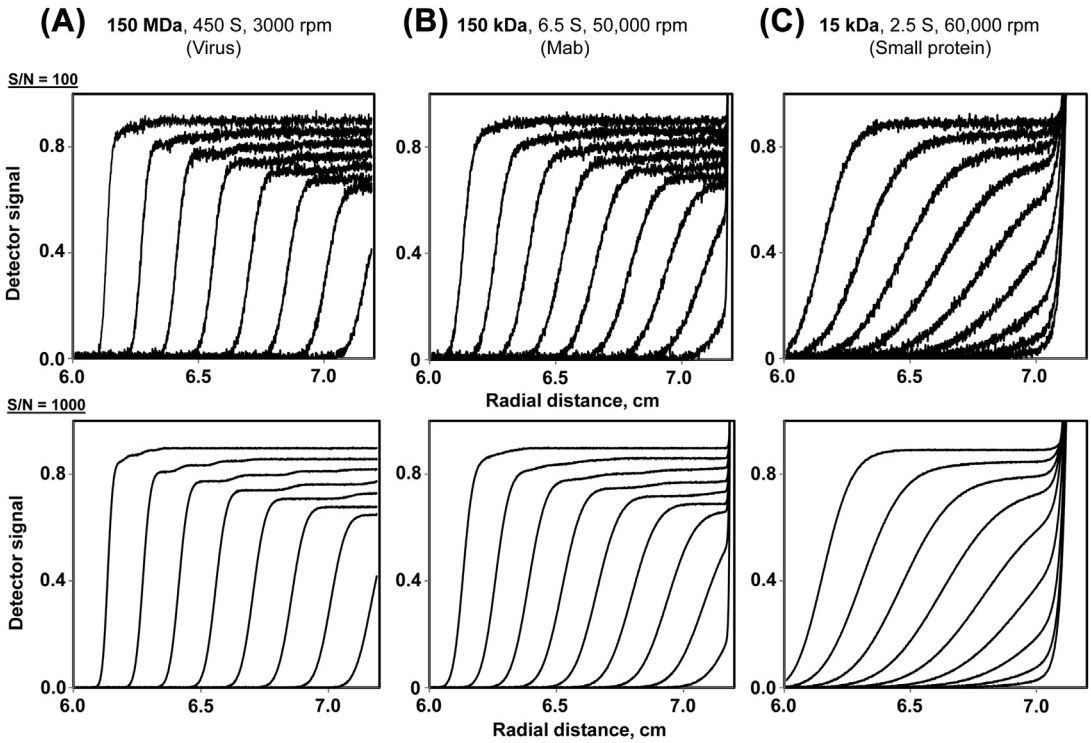

FIGURE 9.4 The impact of sample MW (A-C) and detector S/N (top row = 100 vs bottom row = 1000) on visually (qualitatively) detecting the presence of aggregates in a sample during SV-AUC as revealed via simulated experiments (calculated using SEDFIT). Three samples, each containing the same amount of discrete stable aggregated material (3% dimer + 2% trimer + 1% tetramer) were simulated, but with different monomer masses. (A) virus having a monomer mass of 150 MDa with an *s* value of 450 S run at 3000 rpm, (B) monoclonal antibody having a monomer mass of 150 kDa with an *s* value of 6.5 S run at 50,000 rpm, and (C) a small protein having a monomer mass of 15 kDa with an *s* value of 2.5 S run at 60,000 rpm. The molar masses assigned to each aggregate were based on the monomer mass, while aggregate sedimentation coefficients were assigned based on ratios relative to monomer of 1.5 for dimer, 2.0 for trimer and 2.44 for tetramer [114]. These results show that increased S/N and MW provide for greater visualization and therefore would likely lead to an improved ability to quantify the actual levels of the different aggregate species present.

quantification of this signature in the protein drug's formulation buffer under the working conditions and concentrations of their long-term storage, their actual dosing solution, and potentially even in their in vivo condition after administration to the patient. Such information is important in establishing the consistency of manufacturing each protein drug and for assuring that certain forms of heterogeneity (e.g., aggregates) are kept below a specified limit. The ability to demonstrate this is critical in achieving drug approval or regulatory consent to manufacturing changes either during clinical development or postmarketing. Hence AUC can play an important role in establishing this consistency by revealing potential changes in the heterogeneity and in assessing its impact on the HOS of these drug molecules.

9.5.4 Determining a Sample's Distribution of Sedimentation Coefficients in Order to Assess Its Level of Heterogeneity via Boundary SV-AUC: Using Data Analysis Methods that Do Not Directly Fit the Raw Data to Solutions of the Lamm Equation

Based on the discussion in the previous section, SV-AUC experiments carried out on protein biopharmaceuticals will be influenced to some level by their heterogeneity. Hence the experimentally recorded AUC data scans obtained over the same range of radius values will be the sum of the individual sedimentation profiles of all the different forms of the protein drug molecules present in solution. As a result, if one uses the correct boundary position, r_{srsm}, for each data scan and plots this data vs time, the resulting sedimentation coefficient obtained will correspond to the weight-average sedimentation coefficient, s_w, for the entire sample. Although s_w values can provide very useful information about the nature of the heterogeneity of a protein drug, especially in terms of concentration-dependent self-association (as we will see in Section 9.5.6.2), the level of information provided by this parameter is very limited. What we are really interested in is a plot of the amount of protein drug material with sedimentation coefficients between s and $s + ds$ as a function of sedimentation coefficient. Such information is provided by the differential distribution of the sedimentation coefficients $c(s)$. Such $c(s)$ distributions will look very much like an SEC chromatogram, but with an x-axis in Svedbergs rather than elution volume, and with species eluting in reverse order relative to SEC, with the smaller-size protein species appearing first (at lower s values) followed by the larger-sized proteins (see Figure 9.5)

Over the years various methods for extracting plots of the distribution of sedimentation coefficients of a sample from SV-AUC experiments have been developed. In most cases these methods have assumed that the diffusion coefficient (D) for all the species present in a sample is zero in order to simplify the derivation of the sedimentation coefficient distribution. In this approach the spreading of the migrating sedimentation boundary due to diffusion is in principle not distinguished from that due to the sample's heterogeneity. A very early use of this approach involved simple numerical differentiation of the concentration boundary of the AUC data scan recorded at time t as a function of r to obtain dc/dr values across this boundary, or the direct measurement of the dc/dr profile using a Schlieren optical system. Coupling this dc/dr measurement with appropriate transformation and corrections yielded the apparent differential distribution of the sedimentation coefficients, $g(s^*)$ [47]. For extremely large macromolecular assembles (such as viruses or subcellular structures and their aggregates) this approximate approach may not incur that much of an error (due to the small D values of this material), enabling one to extract a fairly reasonable picture of the sample's actual heterogeneity [48]. A more recent modern improvement in this approach to compute distributions of sedimentation coefficients from AUC data uses the derivative dc/dt instead of dc/dr. In this modern approach the calculation of dc/dt is achieved by taking differences between appropriately closely spaced paired sets of data scans to assess $\Delta c/\Delta t$ to approximate dc/dt. The individual dc/dt curves from multiple pairs of scans are then averaged and then appropriately transformed and corrected to yield the $g(s^*)$ distribution. This approach does a much better job in assessing $g(s^*)$ by significantly reducing experimental noise [19]. Although this approach also suffers from the same intrinsic broadening effects of diffusion, because it produces must better quality $g(s^*)$ data (higher S/N ratio), this allows

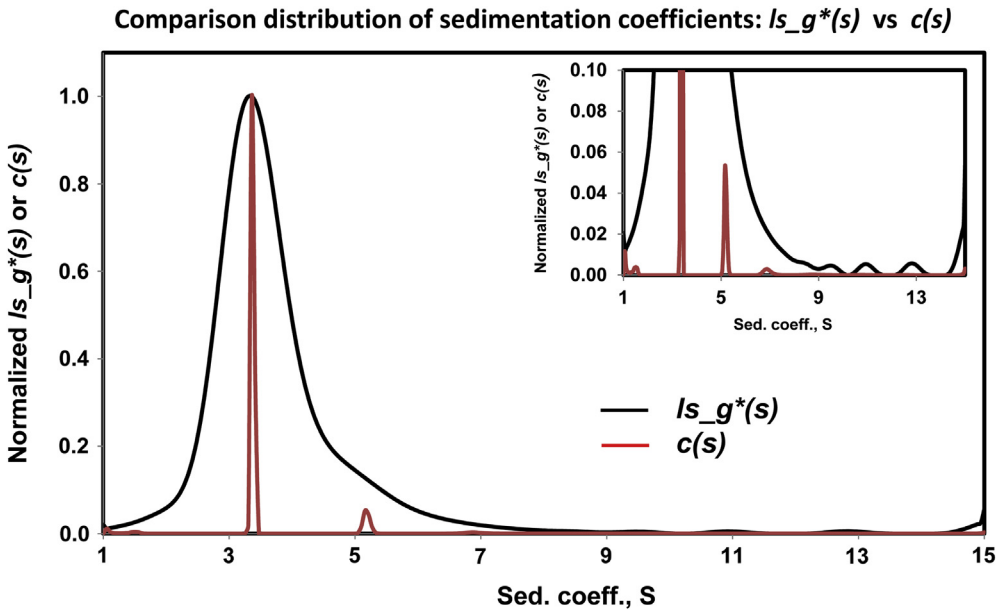

FIGURE 9.5 Distribution of sedimentation coefficients calculated from a boundary SV-AUC experiment on a 66 kDa protein at 1 mg/mL, 20 °C, 45,000 rpm using SEDFIT. Distributions were calculated using *ls_g*(s)*, shown in back, and *c*(*s*), shown in red, analysis. Calculated distributions were then normalized by dividing the original distribution data by the maximum *ls_g*(s)* or *c*(*s*) data point so that the peak maximum for each distribution was equal to 1. Insert plot corresponds to same plot with the y-axis amplified a factor of 10.

more information to be extracted from the detailed diffusion-broadened shape of the sedimenting boundary to obtain information about the diffusion coefficient and MW properties of the sample molecules [19]. This latter approach is implemented in AUC analysis software called DCDT [49,50] or in a modified version called DCDT+ [51], which are available free on the internet from various sites [52].

Another approach for assessing the problem of sample heterogeneity that does account for diffusional broadening of the boundaries is the graphical method developed by van Holde and Weischet (called the vHW method), which was initially described by van Holde in 1978 [53], and more recently improved by Demeler and van Holde in 2004 [54]. In this approach the unique differences between the time dependence of the contributions of diffusion and sedimentation to the boundary spreading process during SV-AUC is exploited. The diffusion contribution to boundary spreading proceeds as a function of the square root of time, while boundary spreading due to sedimentation is a linear function of time. As a result, by extrapolating the same appropriate segmented regions of the migrating sedimentation boundary (as shown in Figure 9.6(A)) obtained from a collection of SV-AUC data scans to infinite time (as shown in Figure 9.6(B) and (D)) the contributions to boundary spreading from diffusion are effectively eliminated. This is done by first characterizing each scan by the term $c(r)/c_p$ (called boundary fraction), where c(r) is the concentration of material in the migrating boundary of a data scan at some fixed time at radial position *r* and c_p is the sample concentration in the plateau of that same data scan. Then the positions of the

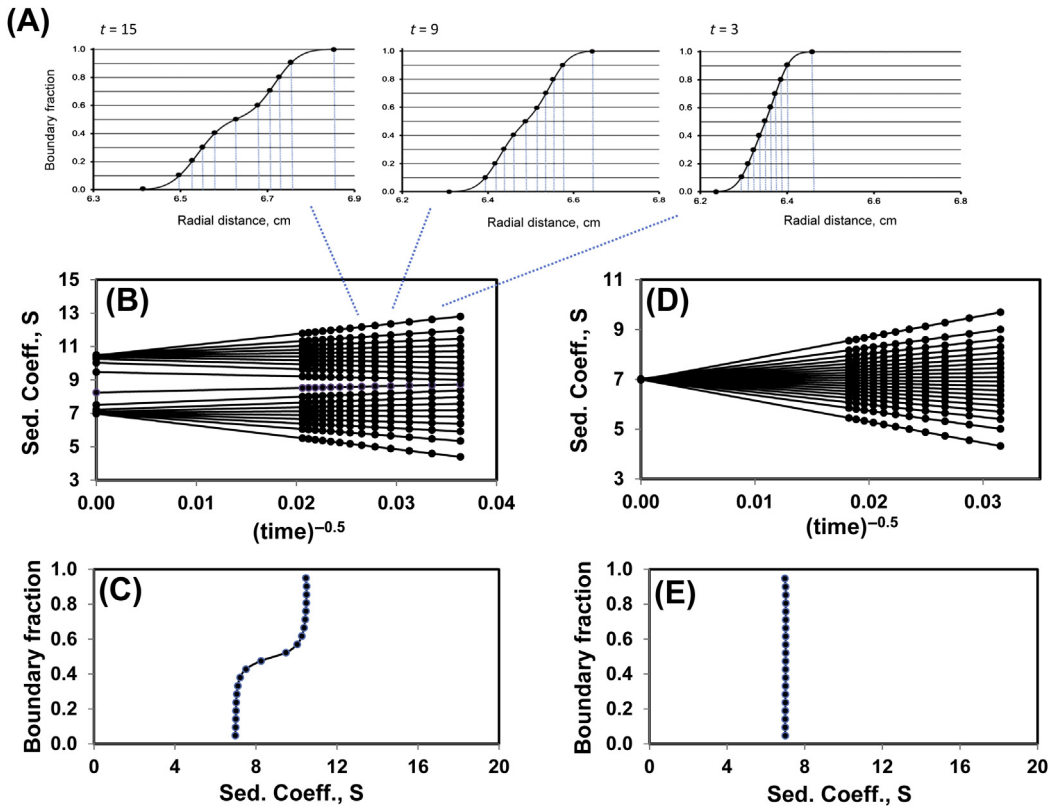

FIGURE 9.6 The vHW analysis plots of simulated idea boundary SV-AUC data for a homogeneous 150 kDa protein having a sedimentation coefficient of 7 S (D & E) and aggregated sample of this material containing 50% dimeric material, which has a sedimentation coefficient of 10.5 S (A-C), at 50,000 rpm. Each data scan used in the analysis was analyzed by dividing its boundary into 20 equal parts as shown in (A) (note: for graphical clarity, however, only every other fraction is actually shown in these plots. In addition, for each plot in (A) the data scans were normalized by dividing data in each scan by the plateau value so that plateau reading on the y-axis was equal to a value of 1). The sedimentation coefficient of each boundary fraction was then calculated using its radial position as a function of time when the scan was recorded. These sedimentation coefficients for each scan were then plotted as the reciprocal of the square root of time and extrapolated to infinite time as shown in (B) for the aggregate containing protein sample and (D) for the homogeneous sample (note: only every 3rd scan was plotted in these plots). The extrapolated sedimentation coefficients values at infinite time were then plots as a function of boundary fraction to yield the integrated distribution of sedimentation coefficient plots shown in (C) for the aggregated sample and (D) for the homogeneous sample.

boundary segments is converted to an apparent sedimentation coefficient, s^*, and these sets of values are plotted vs $1/[t]^{0.5}$. Then the sets of values for each boundary segment are fitted to a line to extrapolate to the origin ($t = \infty$). From this procedure one should in principle obtain the sedimentation coefficient value for each region in the migrating boundary that is free of the effects from diffusion. On plotting these extrapolated sedimentation coefficient values (expressed in Svedberg units) vs $c(r)/c_p$ the resulting plot will yield the integral distribution of the sedimentation coefficients, $G(s)$ for the sample. For a

homogeneous sample this integral distribution of sedimentation coefficients would generate a prefect vertical line positioned over the x-axis at a position corresponding to the correct sedimentation coefficient of the homogeneous sample as shown in Figure 9.6(E). For a heterogeneous sample, this plot would deviate from a vertical line, as shown in Figure 9.6(C). AUC analysis using this specific approach is fully implemented in the AUC software called ULTRASCAN [52,55]; it can also be found in SEDFIT [56], but may not be as fully optimized in performance as it is in ULTRASCAN.

Although these above approaches for assessing the heterogeneity of a protein biopharmaceutical by generating the distribution of sedimentation coefficients of the samples, have the advantage of being free of any specific model or assumptions about the characteristics of the sample, and proceed via fairly simple (relatively speaking) mathematical operations or graphical manipulation of the recorded AUC data scans, the resolution of the information that is obtained by these approaches is limited. In addition, in using these approaches careful consideration must be given to selecting the data scans that are used, which limits to some extent the use of the full set of AUC data scans normally acquired during a complete SV-AUC experiment [49,51,53–55]. Nevertheless, these forms of SV-AUC analysis have been useful and can still play a useful role in SV-AUC analysis especially as a first pass in proceeding to more advanced data analysis programs.

9.5.5 Determining a Sample's Distribution of Sedimentation Coefficients in Order to Assess Its Level of Heterogeneity via Boundary SV-AUC: Using Data Analysis Methods that Do Directly Fit the Raw Data to Solutions of the Lamm Equation

Today more sophisticated modes of analysis of sedimentation data that involve whole boundary modeling are employed that take full advantage of today's much greater computer power to extract potentially more useful and informative information from SV-AUC experiments. The basis of these newer modes of SV-AUC analysis rest on directly fitting the raw SV-AUC scans to solutions of the Lamm equation, Eqn (9.5), developed by Lamm in the late 1920s [57]:

$$[\partial f(s,D,r,t)/\partial t]_r = (1/r)\{\partial/\partial r[Dr(\partial f(s,D,r,t)/\partial r)_t - s\omega^2 r^2 f(s,D,r,t)]\}_t \tag{9.5}$$

The solution, $f(s,D,r,t)$, to this equation for a homogeneous protein having a diffusion coefficient, D, and a sedimentation coefficient, s, will describe the complete sedimentation process of the protein as a function of time, t, and radial position, r, inside in a sector shape centrifuge cell under ideal solution conditions (where there are no significant concentration-dependent or pressure effects) and constant temperature and rotor speed, ω. Experimental conditions that satisfy these solution ideality requirements can usually be achieved in aqueous protein solutions at a concentration of about 1 mg/mL or less where the ionic strength is at least several 10s of mM. Hence, if the correct values for D and s for a protein molecule of interest are known, the normalized analytical solution to Eqn (9.5), $f(s,D,r,t)$, along with the sample's initial concentration, c_0, can be used to calculate the complete set of theoretical data scans, $c(r,t)_{\text{theo}}$, that would correspond to the experimental data scans, $c(r,t)_{\text{exp}}$, acquired during the an AUC experiment. Hence, if there is no experimental noise,

the protein drug is truly homogeneous and the D and s values are accurately known, then on comparing $c(r,t)_{\text{theo}}$ to $c(r,t)_{\text{exp}}$, the following should be true:

$$c(r,t)_{\text{exp}} = (c_0)f(s,D,r,t) = c(r,t)_{\text{theo}} \tag{9.6}$$

Hence the sum of squared differences between $c(r,t)_{\text{exp}}$ and $c(r,t)_{\text{theo}}$ data for all data points should equal zero for all data scans in an SV-AUC experiment, see Eqn (9.7):

$$\sum_t \sum_r \left[c(r,t)_{\text{exp}} - c(r,t)_{\text{theo}}\right]^2 = 0 \tag{9.7}$$

If, however, one does not know the correct values for D and s for the protein molecule of interest, one could attempt a computerized search via the use of appropriate mathematical tools to find the correct D and s values that satisfy Eqn (9.7). Unfortunately, the following factors make this a difficult problem:

1. *Closed analytical functions (solutions) to Eqn (9.5) do not exist.* Nevertheless, approximate analytical solutions having sufficient accuracy to use as fitting functions exist for the ideal solution conditions discussed above and a few other special situations. With increased computing power, more general approaches using numerical integration of the Lamm equation have been developed and implemented which can handle real-world complexities such as: (1) the compressibility of the solvent, (2) the fact that the rotor does not instantaneously reach the final run speed, (3) gradients of density and viscosity within the centrifuge cell arising from sedimentation of sugars, polyols, or other excipients, and (4) even association−dissociation reactions occurring during the run.
2. *In reality all protein biopharmaceuticals contain a certain level of heterogeneity (as we have mentioned in earlier sections of this chapter). They are not homogeneous. Hence this level of heterogeneity needs to be characterized (especially aggregation).* As a result Eqn (9.6) needs to be converted to the following: a linear superposition of n Lamm equation solutions, one for each of the i species present, times the concentration of that species (c_i, its partial concentration) in the protein drug sample as indicated in Eqn (9.8):

$$c(r,t)_{\text{exp}} \cong \sum_i^n c_i\left[f(s,D,r,t)_i\right] = c(r,t)_{\text{theo}} \tag{9.8}$$

   Note that in writing the total concentration as this simple summation it is being assumed that the n species migrate independently of each other during the SV-AUC experiment.
3. *All experiments do have experimental noise. Hence if one conducts a computerized search this search will also attempt to fit the noise, which will make one's ability to find the correct number of species in the sample, and the best partial concentrations and* D *and* s *values for each species, difficult if not impossible.* In trying to calculate sedimentation coefficient distributions there can be multiple solutions having different numbers of species, n, which give equally good fits of the data, and it can be hard to distinguish which minor species might simply be artifacts due to the noise in the data (false peaks). To deal with this problem one can introduce specialized mathematical tools called regularization that constrain the best fit by adding additional criteria, such as that the size distribution should be smooth rather than "spiky."

As a result using Eqn (9.8) instead of Eqn (9.6), Eqn (9.7) now needs to be converted to Eqn (9.9) where instead of equaling zero, it now needs to be minimized to some set confidence limit (which ideally corresponds to the true intrinsic noise in the raw data):

$$\sum_t \sum_r \left[c(r,t)_{\text{exp}} - c(r,t)_{\text{theo}}\right]^2 = \sum_t \sum_r \left\{\left[c(r,t)_{\text{exp}} - \sum_i c_i\left[f(s,D,r,t)_i\right]\right\}^2 = \text{Minimized} \tag{9.9}$$

An array of analytical data analysis programs now exist that take various approaches to finding sedimentation coefficient distributions via direct least-squares fitting using Eqn (9.9). Probably the simplest approach involves using Lamm solutions that correspond to nondiffusing species (assuming $D = 0$ for all species). The analyst first defines an array of possible sedimentation coefficient values (for example 100 different values) between some predefined upper and lower limits, and then the least-squares fitter finds the set of concentrations for each of those 100 species that best fits the experimental data scans. The apparent differential distribution of the sedimentation coefficients obtained by this direct-boundary modeling approach (where the modeling is based on the fact that $D = 0$) is implemented in the software program SEDFIT and is referred to as *ls_g*(s)* analysis [58]. In finding this best-fit size distribution use is also made of algorithms designed to remove known types of systematic (nonrandom) noise in the raw data scans [59] and also regularization techniques [59–62]. The distribution of sedimentation of coefficients generated from this software package generally closely resembles the $g(s^*)$ distributions derived via the dc/dt approach discussed above, despite the totally different approaches used in conducting noise reduction and data analysis. However the *ls_g*(s)* approach puts fewer restrictions on which data scans can be used in the analysis (a two- to threefold larger portion of the total scans can be used relative to dc/dt analysis), which results in a higher S/N ratio for the calculated distribution. However since the actual diffusion coefficients of most protein pharmaceuticals are high enough to significantly broaden the sedimenting boundaries, a danger of incorporating a high fraction of the total scans (a high portion of the total boundary movement) into the fit is that the *ls_g*(s)* algorithm can generate false peaks (because the fitting model cannot provide a good fit since it neglects diffusion) [51].

For both *ls_g*(s)* analysis and *g(s*)* analysis the peaks from a single species are, for the most common size protein drugs, fairly broad (even though the species has a unique sedimentation coefficient, it appears to have a spread of values). This however is not surprising given that these methods do not take into account diffusion. The diffusional broadening results in low resolution (fairly poor separation of different species), making detection and quantitation of minor species rather limited, especially for protein species that migrate with sedimentation coefficient values that are close to the other peaks and/or are present at low levels. Nonetheless these methods can quantitate the sedimentation coefficient for the major peak(s) with high precision, and because the diffusional information has not been removed from the *g(s*)* curves it is possible to fit them with appropriate theoretical models and thereby obtain the buoyant mass of that species with a precision of 1% [63].

Another model using Eqn (9.9), commonly referred to as discrete mixture analysis, takes advantage of prior knowledge concerning the number of species that are actually present in a

sample. Discrete mixture analysis does explicitly model the diffusion coefficient of each species. Those D values can directly be treated as fitting parameters, but often it is more convenient to instead use the molar mass of each species as the fitting parameter, and then internally calculate D from the molar mass and sedimentation coefficient using the Svedberg equation (Eqn (9.4)). Discrete mixture models actually provide better precision for the molecular parameters and concentration of each species than any of the other analytical algorithms discussed here, with statistical approaches that can provide fairly robust 95% confidence limits for all of those fitting parameters. However the most significant limitation of this approach is that it requires prior knowledge (or at least an explicit assumption) of the number of species that are present in the sample. The maximum number of species that can be uniquely fitted will depend on whether they are widely separated in sedimentation coefficient and on their species fractions (it is generally difficult to fit multiple species present at levels near 1–2% or less). When all species are present in roughly equal amounts it may be possible to fit up to perhaps six of them, but when some are present at low levels and/or poorly separated only two or three may be possible. Providing initial guesses for the species properties which are close enough to allow the fitting algorithm to find a unique global minimum variance may also require some additional prior knowledge concerning rough estimates for the sedimentation coefficients of the species which are present, and possibly also their masses. Such prior knowledge might be derived via other modes of analysis, such as SEC, or often from the other forms of SV-AUC analysis discussed here. In particular, it should be noted that this approach could be especially useful when the aggregation present in a protein sample proceeds simply via multiples of the monomer protein drug, e.g., dimer, trimer, etc. and is again limited to the presence of only a few aggregate species. In this scenario it is possible to further constrain the fitting model since accurate MWs of the possible aggregates can be calculated and then combined with the experimentally computed s values to calculate D for that aggregate via the Svedberg equation. By reducing the number of parameters, which need to be fitted, such "oligomer constraints" can greatly increase the precision of the remaining fitting parameters, and may allow a greater number of species to be fitted. The success of such an approach to determine what aggregate species are in fact present and their actual levels is totally dependent on the accuracy of the prior knowledge! Such approaches are implemented in the programs SVEDBERG, LAMM, SEDANAL, ULTRASCAN, and SEDFIT/SEDPHAT [52].

A far more general (and very popular) approach for analyzing SV-AUC data that gives a high-resolution sedimentation coefficient distribution without any prior knowledge of how many species are present does exist. This method of analysis is generally referred to as $c(s)$ analysis and is widely used in the biopharmaceutical industry. It has been implemented in the AUC software programs developed by Peter Schuck and his colleagues, called SEDFIT [56] and SEDPHAT [45]. The key element in this approach involves an assumption (a model), which allows assigning a unique diffusion coefficient to any value of sedimentation coefficient that may be present in the sample. The assumption made is that all species in the sample have the same hydrodynamic shape (overall solution conformation). That hydrodynamic shape is characterized by an f/f_0 ratio, where f/f_0 is the ratio of the actual translational frictional coefficient, f, of a specific protein species to the translational frictional coefficient value, f_0 that the species would have if it was a perfect sphere with the same volume as the protein species, and if that sphere is not hydrated. Like all the other software approaches discussed

in this chapter, the $c(s)$ method also assumes that all the species in the sample sediment independently (a simple mixture with no chemical reactions or solution nonideality effects).

The assumption that all species have the same f/f_0 ratio allows a diffusion coefficient D to be assigned to each sedimentation coefficient, s, using the following relation:

$$D(s) = (18\pi)^{-1}(2)^{0.5}(kT)(s)^{0.5}\left[\eta < f/f_0 >_{\mathrm{w}}\right]^{-1.5}\left[(1-\overline{v}\rho)/\overline{v}\right]^{-0.5} \tag{9.10}$$

Using Eqn (9.10) enables the diffusion coefficients to be calculated as a function of s via the use of a single optimized weight-average frictional coefficient ratio ($<f/f_0>_{\mathrm{w}}$) that is determined during the actual computerized search. Those s and D values can then be used to generate solutions of the Lamm equation (including diffusion) for use in Eqn (9.9). As in *ls_g*(s)* analysis, the analyst sets a range of possible sedimentation coefficients for the size distribution and the number of points (potential species) within that range, and the fitting algorithms then calculate the best-fit concentrations of all those species repeatedly at different $<f/f_0>_{\mathrm{w}}$ values to find the overall best fit. Finally some form of regularization is then imposed to try to eliminate potential false peaks or features in the computed size distribution. With this approach one can actually generate much higher resolution sedimentation coefficient distribution plots to reveal the heterogeneity of the protein drug sample (hopefully with a minimum probability of introducing artifacts). This approach also allows a lower detection threshold for minor species than is possible with *g(s*)*, *ls_g*(s)*, or vHW analysis. Figure 9.5 shows a comparison between $c(s)$ and *ls_g*(s)* distributions calculated from the same experiment. It should also be noted that there exists within SEDFIT several other variants of $c(s)$ analysis that are not restricted to just one value for $<f/f_0>_{\mathrm{w}}$, or that allow different relationships between the s and D values, or that allow the use of other prior knowledge to constrain the parameter search, thus providing models that may be more appropriate for some samples.

Finally, computerized search approaches involving even more complex procedures [64–67] can be implemented to calculate two-dimensional size distributions, without making any assumptions about the hydrodynamic shape of the species which might be present in the sample. In one form, the horizontal grid of possible sedimentation coefficients is combined with a vertical grid of possible f/f_0 ratios, and the least-squares fitter then tries to calculate the concentration present for each combination of s and f/f_0 in the 2D grid. Those concentration data defining a so-called "$c(s, f/f_0)$" or "2DSA" distribution can then be plotted as a 3D plot or a color-coded 2D "heat" plot to visualize the peaks which are present. This type of distribution therefore allows for the possibility that species having different conformations overlap in sedimentation coefficient. Alternatively the second dimension of the distribution can be the molar mass of each species rather than its f/f_0 ratio, to generate a $c(s, M)$ distribution (allowing multiple M values at each sedimentation coefficient).

The strength of such two-dimensional distribution methods is that the only assumptions made about the properties of the sample being analyzed is that all the species fall within certain ranges of s, f/f_0 ratio, or M (and again that species sediment independently). An important weakness is that because they are so unconstrained, the potential for fitting artifacts and/or results which are physically unrealistic (for example f/f_0 ratios outside reasonable values for a folded protein) is high. Some form of regularization or other procedure to minimize the potential for artifacts is definitely necessary, and sophisticated mathematical and statistical approaches such as genetic algorithms are sometimes employed to try to determine

which species are truly real and necessary to explain the data. These 2D distribution approaches require far more computer power (in terms of both processing time and storage) than any of the others discussed here, and often involve the use of remote supercomputers or dedicated local high-performance computer clusters using many processors in parallel. Such resources are presently available online through the University of Texas Health Science Center at San Antonio, Texas using the program ULTRASCAN. However, most biotechnology companies are understandably reluctant to send their proprietary data through the Internet to access supercomputing resources, or to invest in their own high-performance computing clusters. Further, the intense computing requirements make it difficult for the analyst to explore all the potential choices and fitting options that might affect the analysis outcome.

Overall in the opinion of the authors, these 2D distribution methods are potentially useful for analyzing biotechnology products, but it is unclear whether they are qualified for pharmaceutical use. The academic literature suggests that they can successfully identify individual components within mixtures containing roughly equal parts of perhaps four to five major species. However these methods have not yet been rigorously tested with respect to either (1) the extent to which they generate false species or other types of analysis artifacts, or (2) their ability to detect or quantify small amounts of minor species such as aggregates, let alone to correctly identify the molar mass of such species.

9.5.6 Assessing Aggregation via Boundary SV-AUC

A major concern when producing a protein biopharmaceutical is monitoring and minimizing the propensity of these important potential drugs to aggregate. It has already been said in this chapter that AUC can play a significant role in this area. The following section focuses on understanding how SV-AUC in particular can contribute in this area.

9.5.6.1 Limit of Quantitation (LOQ) in Measuring Aggregation

Probably the most common and important use of AUC in product development within the biopharmaceutical industry today is for assessing the amount and size distribution of aggregates in protein biopharmaceuticals. Although this information is routinely measured by using SEC (as discussed in Chapter 7 in this book), it is known that SEC has important limitations and can provide misleading information about the true level of aggregation present in a sample [23,68–70]. Of key concern in this area is the interaction of the injected SEC sample with the enormous surface area provided by the chromatographic material present in the SEC column [71]. One consequence of such interactions is degraded chromatographic resolution, making appropriate quantitative integration of the resulting SEC chromatogram difficult. A far more detrimental outcome is the preferential removal of specific variant forms of the protein drug from the resulting SEC chromatogram, which in the most serious case is the selective removal of aggregated material from the SEC chromatogram. Given the large surface area accessable to a protein and even its largest aggregates as it migrates through the SEC column, the presence of even very low levels of binding sites on the chromatography particles will require the biopharmaceutical scientist to take steps to overcome this problem. Several ways to achieve this (beside scanning the chromatography landscape for a SEC column made with chromatography material that does not interact with the various forms of the protein drug of interest) are: (1) use a SEC

mobile phase that itself inhibits the bind of protein drug and its various forms to the surfaces of the chromatography particles, but does not alter the level of aggregation or its distribution of sizes [68]; (2) pretreat the SEC column with multiple injections of the sample material that will be commonly tested on the column or with some other common inexpensive protein such as BSA to hopefully saturate the binding sites (which may need to be repeated periodically); or (3) a combination of both.

By using SV-AUC to assess aggregation, however, a number of benefits are immediately realized. These include: (1) virtually no method development; (2) a negligible level of surface contact area in comparison to SEC; (3) the ability to assess the aggregation level in the exact matrix the protein drug is in (its formulation or process intermediate buffer); and (4) the ability to cover a much larger range of aggregate sizes than SEC. As a result, SV-AUC can be an extremely useful analytical tool to assess aggregation during the early stages of a protein drug project until an adequately functioning SEC method has been developed, as well as an important orthogonal method to support the SEC's qualification and eventual validation. Indeed it is now routine for regulatory authorities to ask for SV-AUC to be used to cross-qualify SEC protocols.

However, the major limiting factor in using AUC in this area concerns a clear understanding that the LOQ of SV-AUC is much higher than a correctly working SEC method, where the LOQ is somewhere around 0.1–0.5% in terms of percent total aggregation [23,32]. In the case of SV-AUC when using $c(s)$ analysis in SEDFIT (which we have already indicated is the most common approach used today to assess aggregation via SV-AUC analysis) the initial work by Schuck and colleagues using simulated data stated that the levels at which aggregation could be detected reliably is about 0.2% for a detector system having a S/N value of 200 [72,73], while Gabrielson et al. [36] estimated an LOQ of 0.6%, again using simulated data. However, a number of reports have appeared from various biopharmaceutical scientists pointing out that in practice the experimental LOQ for small oligomers (dimer to tetramer) falls more within the range of 1–3%, when using the UV-VIS detector [23,33–38,74]. Unfortunately the upper part of this range is where concern starts to appear that a protein drug could be showing signs of an aggregation problem. After re-evaluation, again with simulated AUC data, Schuck [74] estimated LOQ when using $c(s)$ to range from ~0.6% to 2% when using regularization confidence levels of 0.68 and 0.95, respectively (with the former being the most common confidence level being used in the field). At present, it is the authors' experience that the LOQ most likely falls closer to 2% (using the UV-VIS detector). It is also worth noting that the variability in results for low-level minor species among replicate samples does not appear to follow random statistics. Some replicates will give results in close agreement (consistent with the random noise in the raw data), while other replicates will differ much more widely, often by showing higher levels of aggregates and additional aggregate species. The fact that in practice the LOQ for detecting aggregates is significantly higher than it should be based on realistic simulations would seem to indicate that experimental AUC data are plagued by the presence of small, but variable sources of systematic errors. The possible sources of these systematic errors will be discussed in more detail below.

The fact that SV-AUC often does not have the sensitivity and reproducibility to quantitate the low levels of aggregates that are typically present in therapeutic proteins (especially those in late stage development) is actually not an impediment to using SV-AUC to cross-check (cross-validate) results from SEC. For that purpose it is both possible and desirable to

use stressed (force-degraded) samples that contain higher levels of aggregates (above the LOQ for SV-AUC, so quantitative comparisons can be made). For this purpose, one should challenge the SEC protocol with the types of samples for which it is most likely to produce poor results: samples containing larger aggregates, or aggregates which are more denatured, and hence are more likely to be filtered out by the column. The use of multiple types of stress (oxidation, heat, agitation, UV exposure, *etc.*) to potentially produce different types and size distributions of aggregates has been recommended by regulatory authorities.

Unfortunately the major factor limiting the ability of SV-AUC to quantify low levels of aggregates is actually not the signal/noise ratio of the raw data, it is instead systematic errors related to the initial quality (and degradation during usage) of the AUC cell components used in the field, or correctly orienting those AUC cells in the rotor [33]. One significant problem is the uncertainty in the accuracy of a hierarchy of radial alignments of various pieces of AUC hardware so that the walls of the sector-shaped sample compartment are precisely parallel to the centrifugal force, which is critical to avoiding convective transport during SV-AUC. If convection does occur it generally results in falsely high apparent levels of aggregates (often including false aggregate species) [33]. Those cell alignment issues include the following:

1. Correct alignment of the scribe lines on the rotor holes and on the bottom of the AUC cell housing to the center of rotation of the rotor and center of the AUC cell respectively. Note that on some rotor holes the inner and outer scribe lines do not agree with the inner and outer scribe lines on the AUC cell housing bottom (if these scribe lines were made correctly they would coalign).
2. Correct alignment of the scribe lines on the bottom of the AUC cell housing with the alignment key inside the cell housing. In addition, the two slots located on the bottom of the cell housing, which are used by both the cell alignment tool made by Spin Analytical and the "Amgen tool" [33] to align the AUC cell in the rotor, must also be aligned exactly 90° from the position of the key inside the cell housing.
3. Properly sector-shaped compartments ("channels") that are also properly aligned with the keyway slot on the centerpiece so the compartment side walls are radially aligned with the center of rotation of the rotor.

Additional quality issues with the cell centerpiece are that the walls of the internal sample and reference channels must be smooth and free of ridges, scratches, or other defects that would cause the sedimenting molecules to accumulate along the wall, increasing the local solution density, which could then trigger convection (see section 9.5.1). Such defects may exist in newly purchased centerpieces, or may develop during normal usage, so careful inspection by the analyst before each use is essential. Further, if the cell leaks during the run and the fill volumes of the sample and reference channels become substantially different, the rib (septum) that separates these channels may become permanently bowed, which will cause convection. Such bowing is unfortunately quite difficult for the analyst to detect without special measurement tools. Bowing of the septum might also develop over time after extensive usage, but whether that really happens in the absence of any leakage is unclear. Finally, manufacturing issues concerning uneven shrinkage during manufacturing of the commonly used epoxy filled (Epon) centerpieces as noted by Kirschner and Schachman [39] might represent another source of systematic errors.

Until these factors are adequately controlled and their full impact understood, it is not likely that any additional improvements in analysis software applied to suboptimal SV-AUC raw data will lead to any significant improvement in the reproducibility or LOQ for assessing aggregation via SV-AUC. Hence SV-AUC measurements of samples run in singlet will be used more as a coarse insurance tool to avoid crude or gross errors that can occur with SEC methods when more than about 2–3% of aggregates are filtered out by the column. Greater sensitivity, when needed, can of course be obtained by running replicate samples by SV-AUC and averaging the results.

Hopefully the needs of the biotechnology industry will drive future improvements in the manufacturing quality and fabrication of AUC components [35] to improve the alignment issues mentioned above, and possibly the development of better UV-VIS and interference detectors [75] that provide higher S/N and lower systematic errors. In the meantime, the following suggestions may have some merit for helping the experimenter in assessing and potentially improving SV-AUC's ability to measure low levels of aggregation:

1. Establishment of a stable, rugged, and well-characterized protein reference standard with an accurately known level of aggregation (known with an uncertainty ±1% or better) to help assess AUC hardware and methodology for measuring aggregation. Such a standard would also be useful for analyst qualification and for routine tests of proper instrument performance. The authors would like to note that the establishment of such a standard might represent a worthy project for a federally funded organization like National Institute of Science and Technology (NIST) to develop or worthy commercial opportunity for some company.
2. Investigate the potential use of difference boundary SV-AUC with the Rayleigh interferometer in which the same stable protein sample is placed in both sectors of a centerpiece to evaluate centerpiece quality and optical alignment problems. Such assessments could be feasible by measuring the term $\Delta s/s$ using Eqn (9.4) in reference [39]), which for correctly made components and aligned hardware should be effectively zero. Hence this methodology may provide a sensitive in-house procedure for assessing the quality and alignment of AUC hardware components, to evaluate when historical usage has negatively impacted cell hardware (requiring replacement), or to determine when poorly made AUC hardware components have been purchased [39]. See Section 9.9.2.2 for further discussion on difference boundary-SV.

Other experimental factors and conditions that can influence the ability to detect and quantitate low levels of minor components are:

1. The choice of whether to use the 4-hole or 8-hole rotor (3 samples maximum per run or 7 samples maximum per run for UV detection). The use of the 8-hole rotor greatly increases throughput, but with UV detection the number of scans that can be acquired and analyzed is severely limited, reducing the sensitivity and reliability of the results.
2. The quality of the detector (its S/N ratio, its linearity, and the accuracy and linearity of the readout of the radial positions).
3. The choice of rotor speed. Higher speeds increase the intrinsic resolution of aggregates from the monomer, but also increase the likelihood of artifacts due to convection, and reduce the number of scans available for analysis (signal averaging). The use of higher

speeds also limits the ability to detect and quantitate very large aggregates (because they sediment too quickly to be detected), especially when running 7 samples in the 8-hole rotor.

4. The number of replicate samples used to calculate average aggregation level of a sample, and whether those replicates were measured in the same SV-AUC run or different SV-AUC runs.

9.5.6.2 Detecting Aggregation Involving Reversible Concentration-Dependent Self-association

One of the key points in assessing the aggregation of a protein biopharmaceutical is understanding what aggregates are present in its formulated state as a DS or DP. In general SEC analysis is carried out by injecting samples that are at concentrations that are fairly low (typically 1 mg/mL), which are then substantially further diluted during SEC chromatography. Also in many (if not most) cases the SEC protocol employs a mobile phase that is significantly different from the actual formulation buffer of the DS or DP. Therefore typically during SEC chromatography the injected sample experiences changes in the sample buffer matrix as well as further reduction in protein concentration. Under these conditions SEC's ability to detect reversible concentration-dependent aggregation is greatly reduced (if not entirely eliminated). Although it might be possible to detect the presence of reversible self-association by injecting protein drug samples at different concentrations onto the SEC column to conduct frontal analysis SEC, or by careful monitoring of the monomer peak broadening effects as a function of concentration (see Chapter 7 on SEC in this book), it may not be possible to do this under actual vialed formulation buffer conditions due to interactions of the protein drug with the column matrix under those solution conditions. In addition, injecting samples at very high protein concentrations will potentially produce nonideal chromatography effects that could make assessments of possible self-association very difficult. Hence the highest concentration that could be investigated by this approach is significantly limited, making it an unattractive approach to detect reversible self-association in the biopharmaceutical industry.

A far better and simpler approach to detect the presence of reversible self-association is to conduct SV-AUC runs at different protein drug concentrations. Using the UV−VIS optical system on the analytical centrifuge, along with short 3-mm path length AUC cell, concentrations as high as about 20 mg/mL can be investigated before encountering optical artifacts due to bending of the light beam by the steep protein gradients generated during normal SV-AUC (Schlieren effects). Using the Rayleigh interferometer concentrations as high as ~50 mg/mL can be investigated. (Note that these upper limits will depend on the protein molar mass and the rotor speed because those affect the steepness of the boundary.) Simple calculation of the weight-average sedimentation coefficient, s_w, for the entire sample for each run at different concentrations plotted vs the initial concentration of the sample analyzed will classically show s_w to be an increasing function of total protein concentration if the given protein drug displays concentration-dependent self-associating properties, see Figure 9.7(A). In comparison, if a sample does not undergo concentration-dependent self-association, the common outcome is to see a decrease in the values of s_w as a function of concentration. This decrease in s_w with concentration is due to nonideality effects that are present, see Figure 9.7(B). Alternatively, comparing calculated $c(s)$ or possibly $ls_g^*(s)$ vs s plots generated

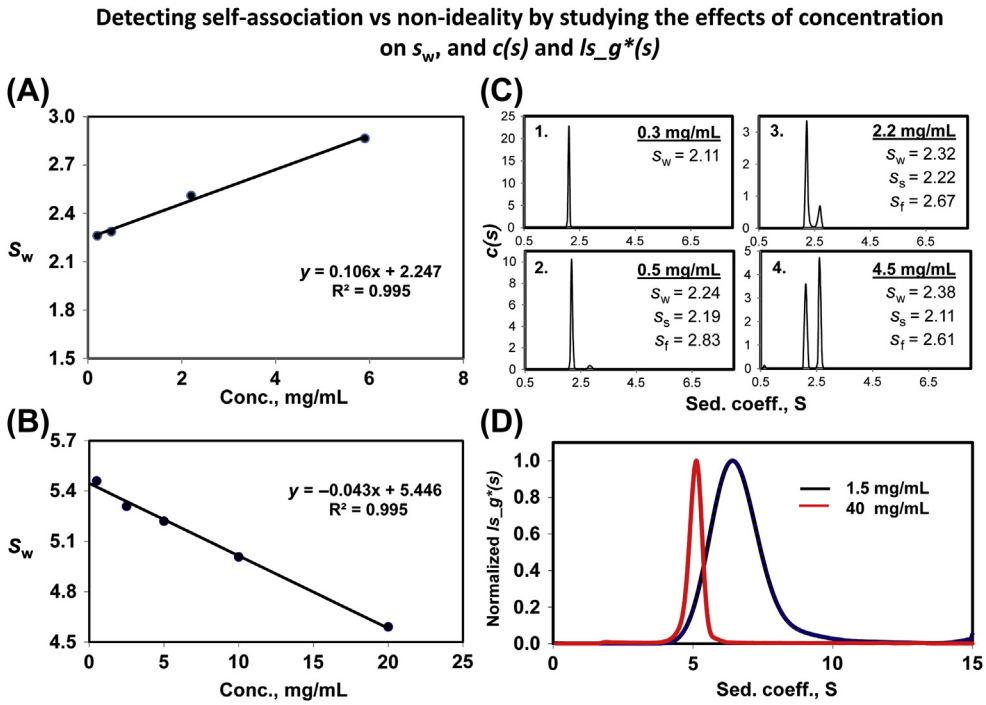

FIGURE 9.7 A plot of the weight-average sedimentation coefficient, s_w, obtained from boundary SV-AUC experiments at different concentrations for a 24 kDa and a 150 kDa protein as a function of total concentration are shown in (A) and (B), respectively. In the case of the 24 kDa protein, the s_w values are observed to increase with concentration. Such a result is a classical behavior for the presence a self-associating system (a system where aggregates increase as the concentration increases). On the other hand in the case of the 150 kDa protein we observe a decrease in s_w with concentration, which is what we would observe due to the presence of nonideality effects, e.g., excluded-volume and electrostatic effects. Using $c(s)$ analysis on another protein-buffer system as a function of concentration (C), reveals self-associating behavior with more detailed information about the system. However, depending on the aggregating properties of the system, e.g., equilibrium constant, rates of association and dissociation, and the reversibility of the aggregation, the $c(s)$ plots can be misleading and easily misinterpreted. When reversible association is present individual peaks may not represent true molecular species, and their positions do not necessarily represent the sedimentation coefficient of a unique species. This arises due to the limitations of the normal $c(s)$ model, which assumes the absence of any self-association. In these situations, proper data interpretation will require much more advanced data modeling to be used. The data plot in (D) shows the use of $ls_g^*(s)$ analysis in detecting the impact of increasing concentration on a protein system. In this case the protein shows classical nonideality behavior. In this much simpler mode of data analysis, the calculated apparent distribution sedimentation coefficients of the same sample measured at two very different concentrations are presented. In both cases the resulting $ls_g^*(s)$ distributions were normalized by dividing the calculated distribution data by the maximum $ls_g^*(s)$ value, so that the largest peak value in these plots is equal to 1. The resulting data shows the anticipated decrease in sedimentation coefficient with increasing concentration, as well as a very significant sharpening of the boundary as indicated by the distribution in red. For systems that display simple nonideality behavior this sharpening of the boundary is classical and is due the slowing of the sedimentation of the sample material at high concentration near and in the plateau region and the increase in sedimentation for material in the trailing part of the boundary. The net effect of both these phenomena is the increased sharping of the boundary and the reduction in the value for s_w as the total concentration of the sample increases.

for the same sample as a function concentration may show the increasing presence of aggregated material, as seen in Figure 9.7(C), or/and a shift and broadening in the monomer peak toward higher sedimentation coefficients. However, independent of whether the protein self-associates, as the protein concentration increases nonideality effects will also increase. The increasing effects of this nonideality will reduce the sedimentation rate of the sample and distort its boundary, due to several effects that are a function of the formulation buffer and the physicochemical properties of the sample [8], see Figure 9.7(D). This opposing nonideal solution behavior can decrease s_w values and distort the shape of the $c(s)$ and $ls_g^*(s)$ vs s plots. Hence depending on the interplay of these opposing effects the presence of concentration-dependent self-association can be completely or partially masked if nonideality effects are not properly accounted for. Although additional AUC experiments can be conducted in an attempt to obtain a better understanding the self-association process, for drug development purposes it is often sufficient to simply (1) establish that significant self-association does exist under relevant process or formulation conditions, and (2) establish whether this association is reversible.

In concluding this section it should be mentioned that although earlier in this section we stated concentration limits for boundary SV-AUC, it should be noted that running the analytical centrifuge at lower speeds (to reduce the steepness of the refractive index gradients that generate adverse optical artifacts) could enable higher concentrations to be probed. However, this ability to probe higher concentrations will come at a cost of reduced separation resolution. Nevertheless, such a loss might be tolerable if the level of concentration that can be reached is significantly improved.

9.6 BAND SV-AUC

Another mode of SV-AUC analysis is band sedimentation velocity (band SV-AUC, see Figure 9.2) [76]. In general this mode of AUC finds its greatest use in characterizing very large strongly UV-absorbing macromolecules structures like DNA and supramolecular structures such as ribosomes and viruses [77]. As a tool in the biopharmaceutical industry it could find good use in characterizing very large drug particles containing proteins used in vaccines and complex drug delivery systems, such as in gene therapy where VLPs, viruses or nanoparticles are used. Some of the advantages of using this technique are: (1) a much lower amount of material is required relative to boundary SV-AUC (only 2–5% of what is needed for a boundary SV-AUC) and (2) the ability to run the samples in different buffer pHs/excipients solutions without the need to buffer exchange since, the sample matrix change occurs during the run as the sample band migrates through the liquid column toward the base of the AUC cell [78,79].

The basic principle in using this technique involves layering a sample solution over a much denser buffer solution. To achieve the layering process in the analytical centrifuge a special band-forming centerpiece is required (see Figure 9.2(E)). In these centerpieces a small hole (or well) is present that is connected to the sample sector via two small channels. The AUC cell is assembled with this centerpiece in the normal manner with the exception that the top window is not put into the cell. With the band-forming centerpiece in place within the AUC cell housing, anywhere from 5–15 μL of sample solution is placed in the sample sector well. The top window is then put in place and the cell is appropriately sealed. At this point

appropriate volumes of the denser solution are added to both the reference and sample sectors. After sealing the filling-hole the cell is placed in the rotor and temperature equilibrated within the centrifuge. During the acceleration phase of the band SV-AUC run the sample is layered out onto the dense solution via the action of the centrifugal field (note: air displaced by the migration of the sample solution into the sample sector will move into sample well via the upper channel connecting both compartments). Initially the sample solution will float on top of the denser solution in the sample sector. Subsequently the diffusion of the denser buffer solution components into the sample solution creates a positive density gradient which needs to be greater than the weak negative gradient created by the migrating sample band (due to the presence of the macromolecule). Overall the idea is to always have a net positive density that runs from the meniscus to the bottom of cell during the band SV-AUC experiment to stabilize the migrating sample band against convective mixing in the centrifugal field (which would occur if a negative density gradient existed anywhere in the solution column). Although higher density solutions are usually made by adding higher concentrations of salt or excipients, the high density can also be achieved by using the same buffer components, but substituting heavy water (D_2O) for H_2O to make the buffer.

In most cases where experiments were being conducted to study the effects of pH, ionic strength or the impact of specific excipients on the protein drug, these experiments would most likely be carried out using heavy water (D_2O) in order to avoid the use of high salt solutions to stabilize the migrating band. However, it should be noted that running protein samples using band sedimentation it can be a bit more of a challenge to find experimental conditions for avoiding convection artifacts. This is due to the higher protein concentration needed to monitor their migration in comparison to stronger UV absorbing biomolecules like nucleic acids, creating a greater demand for a more stabilizing (steeper) density gradient [80].

It should also be noted that due to the higher solvent density and the associated increased viscosity when running protein samples through formulation buffer made with D_2O, proteins will migrate with sedimentation coefficients that will differ substantially from their normal formulation conditions in H_2O formulation buffers. While it should, of course, in principle be possible to correct the sedimentation coefficients to standard conditions in water, in this case doing so accurately is made difficult by the increase in protein mass during the experiment as deuterium exchanges with hydrogen atoms in the protein. Nevertheless, this shift in the observed sedimentation coefficients should not be a significant problem when making comparisons between different lots (e.g., for comparability protocols), or for studies of the effects of ionic strength/pH relative to some standard formulation conditions in D_2O. Finally, under rare conditions it should be pointed out that D_2O could impact the conformation of a protein [81].

In comparison to boundary SV-AUC, band SV-AUC has a much stronger dependence on having a sufficient positive density gradient maintained throughout the run. This stronger dependence is due to the need to overcome the destabilizing effect of the leading front side of the migrating sample band (which is unstable due to its decreasing density with increasing radial distance). Some of the key parameters that influence what magnitude of stabilizing density gradient is needed are the following: (1) the density difference between sample solution and the buffer solution the sample will be migrating through; (2) the volume of sample that will be layered on to the denser buffer solution; (3) the concentration of sample being applied; (4) the rate of migration of the sample; (5) the rate of diffusion of the

component(s) that create the higher density in the buffer; and (6) the rate of acceleration of the rotor. Hence band SV-AUC work conducted in D_2O buffers, particular for proteins, will most likely require more experimental method development in order to achieve stable banding. Details for dealing with these experimental variables to achieve a successful band SV-AUC experiment have been discussed by Vinograd and coworkers [80]. Lastly it should be noted that another major difference between band SV-AUC and standard boundary SV-AUC is that the samples become much more diluted, which often means they must be loaded at higher concentrations to give sufficient signal. Whether this is a drawback depends on whether the goal is to measure rapidly-reversible self-association.

9.7 SEDIMENTATION EQUILIBRIUM, SE-AUC

In SE-AUC much lower rotor speeds are used than in SV-AUC, and we do not want to actually pellet any of the components of the sample. As the sample slowly redistributes and creates a concentration gradient across the cell we can reach a steady state (an equilibrium) where the strength of the centrifugal field just balances the diffusional forces at every position in the cell. When equilibrium is in fact reached, the change in concentration as a function of time, dc/dt, will equal zero at all radial positions in the centrifuge cell. Under these conditions the Lamm equation, Eqn (9.5), can be set equal to 0 and then rearranged and combined with the Svedberg equation (Eqn (9.4)) to yield the equation for SE-AUC under dilute ideal solution conditions, Eqn (9.11):

$$d\ln(c)/d\left(r^2/2\right) = \left[M_w(1-\overline{v}\rho)\omega^2\right]/[RT] \tag{9.11}$$

This equation indicates that at equilibrium for a homogeneous protein solution a single stable exponential concentration gradient will be generated (an exponential function of $r^2/2$ rather than r). By plotting the $\ln(c)$ as a function of $r^2/2$ the slope of this linear plot will yield the MW of the protein molecule independent of its hydrodynamic shape (which plays an important role in SV-AUC experiments). In general it was this mode of sedimentation analysis that was most commonly used many years ago to assess the MW of proteins and their complexes since it was totally independent of the frictional properties of the protein molecule, which made MW assessment via SV-AUC much more difficult. Note also that due to the static nature of an SE-AUC experiment any shape of cell can be used (at equilibrium there is no net transport to collide with the walls of the cell).

9.7.1 Assessing Stable Noninteracting Aggregates vs Aggregation Involving Reversible Concentration-Dependent Self-association

SE-AUC analysis is also an important mode for studying the association properties of a protein by examining samples over a range of concentrations to determine whether M_w increases systematically with concentration due to the law of mass action. When such tests indicate the occurrence of significant reversible association, one can then try modeling the experimental data with various association models (different stoichiometries and equilibrium constants) to determine which model best fits the experimental data. This process

can significantly improve one's ability to decipher the details and energetics of the aggregation scheme [82]. Note, however, that since it involves modeling exponentials there are sometimes multiple models which fit the raw data similarly well (although these ambiguities can often be resolved in combination with SV-AUC or other biophysical techniques).

Although SE-AUC experiments are still conducted to some extent today for studying reversibly self-associating protein systems, especially in conjunction with SV-AUC experiments, biopharmaceutical scientists tend not to employ SE-AUC experiments very often since they require significantly more time to run (often 2–3 days if multiple rotor speeds and standard equilibrium cells are employed), making them rather unattractive in our fast-paced world. Nonetheless SE-AUC is considered the gold-standard tool for quantitatively assessing reversible associations, and can be useful in trying to find solution conditions (formulations) that could potentially minimize this type of aggregation if necessary. In terms of distinguishing between irreversible aggregates vs reversible aggregation/association, that is often best done using SV-AUC. However this distinction can also be made using SE-AUC experiments at different initial loading concentrations and using diagnostic plots of apparent M_w vs concentration [83]. However, in conducting these measurements the impact of nonideality effects must be minimal in order to make the data interpretation clear.

In general, a deep understanding of the details of the association process is typically not the goal of the process biopharmaceutical scientist. Nevertheless, as will be discussed in the next section (9.7.2), SE-AUC conducted using very short sample column heights may prove to be particularly a useful activity for the biopharmaceutical to study the impact of very high protein drug concentrations (in the range of 20–200 mg/mL) on the aggregation propensity of these drugs.

9.7.2 Qualitative Assessment of Aggregation at Very High Protein Concentrations

One area that is attracting a great deal of interest is associated with the need to understand the impact of very high protein concentration (concentrations in the range of 100–200 mg/mL and possibly greater) on the physicochemical properties of protein biopharmaceuticals. This need has arisen as a result of interest in reducing the cost of protein drug delivery by substituting the costly IV delivery in a hospital or doctor's office with patient self-administration via a simple subcutaneous (SC) injection of 0.5–1.0 mL of the protein drug. Keeping the dose volume low enough for SC administration then requires the very-high protein concentrations mentioned in the beginning of this section. At these high concentrations the investigating scientist is dealing with the world of strongly nonideal solution behavior, where interpreting data generated by any biophysical method will be complicated by the presence of a number of significant nonideality effects. In the case of AUC, studying proteins solutions at increasingly higher concentration quickly reduces our ability to accurately generate meaningful quantitative data due to our inability to account for the strong nonideality effects. One important point, however, is that equilibrium methods such as SE-AUC or static light scattering are influenced only by *thermodynamic nonideality*, whereas hydrodynamic methods such as SV-AUC, dynamic light scattering, or rheometry are influenced by multiple *hydrodynamic nonideality* effects in addition to thermodynamic nonideality.

One possible approach for assessing the presence of reversible self-association at very high protein drug concentration could take advantage of simply studying the change in apparent MW of a protein drug as a function of concentration using SE-AUC in a way very similar to that implemented by Minton and coworkers using static light scattering [84–86]. In this approach SE-AUC experiments are carried out in AUC cells using very short column AUC centerpieces (so-called "8-channel" centerpieces, see Figure 9.2(G)) using the Rayleigh interferometer as a detector [87–89], but at very low speeds. This approach offers a number of advantages, which include the following:

1. Due to the very short solution column height used in these experiments, SE-AUC can be achieved in a matter of only several hours. Hence two SE-AUC runs per day could likely be achieved. Using an eight-hole rotor with the Rayleigh interferometer would enable 64 samples per day to be run (since 32 samples per AUC run would be possible).
2. Also, due to the very short column height used in these experiments the concentration at the midpoint between the each sample's meniscus and base, r_{mid}, corresponds to the initial concentration of the sample loaded into the centerpiece hole, c_o [89,90]. Hence by rewriting Eqn (9.10) in a slightly different form we get,

$$(\mathrm{d}c/\mathrm{d}r)(rc)^{-1} = \left[M_w(1-v\rho)\omega^2\right]/[RT] = (\mathrm{d}c/\mathrm{d}r)_{mid}(r_{mid}c_0)^{-1} \tag{9.12}$$

   As a result, measuring the slope $(\mathrm{d}c/\mathrm{d}r)$ of a c vs r plot at r_{mid}, $(\mathrm{d}c/\mathrm{d}r)_{mid}$, then dividing it by $r_{mid}c_0$ will provide the weight-average MW, M_w, value at r_{mid}.
3. Given the low rotor speed no significant fractionation of the protein drug sample should occur. Therefore the calculated M_w should correspond to the entire sample. Hence this should lead to a further reduction of encountering any significant curvature in the c vs r plot making any inaccuracy in assessing r_{mid} of minimal consequence, see Figure 9.8(A). In addition, the low rotor speed in combination with the short column height would also make baseline correction to interference pattern virtually negligible, see Figure 9.8(B).

   Therefore data could readily be generated to create the necessary M_w vs c plot to detect the presence of self-association as outlined by Minton and coworkers for LS measurements (also see Chapter 8) using scaled particle theory to handle the thermodynamic nonideality [91–93].
4. Sample consumption is very low, since the sample volume used is on the order of 15 μL per sample concentration. In addition samples could be recovered if necessary.
5. Radial independent (RI) and time independent noise reduction similar to that developed by Schuck and Demeler [59] could potentially be used to attain more accurate M_w values, especially at lower protein drug concentration.

9.8 DENSITY-GRADIENT SE-AUC

An interesting alternative to the SE-AUC approach, which actually uses high centrifugal fields, is called density-gradient SE-AUC (also referred to as isopycnic SE-AUC). This novel form of SE-AUC is run at very high salt concentrations, which in combination with the high

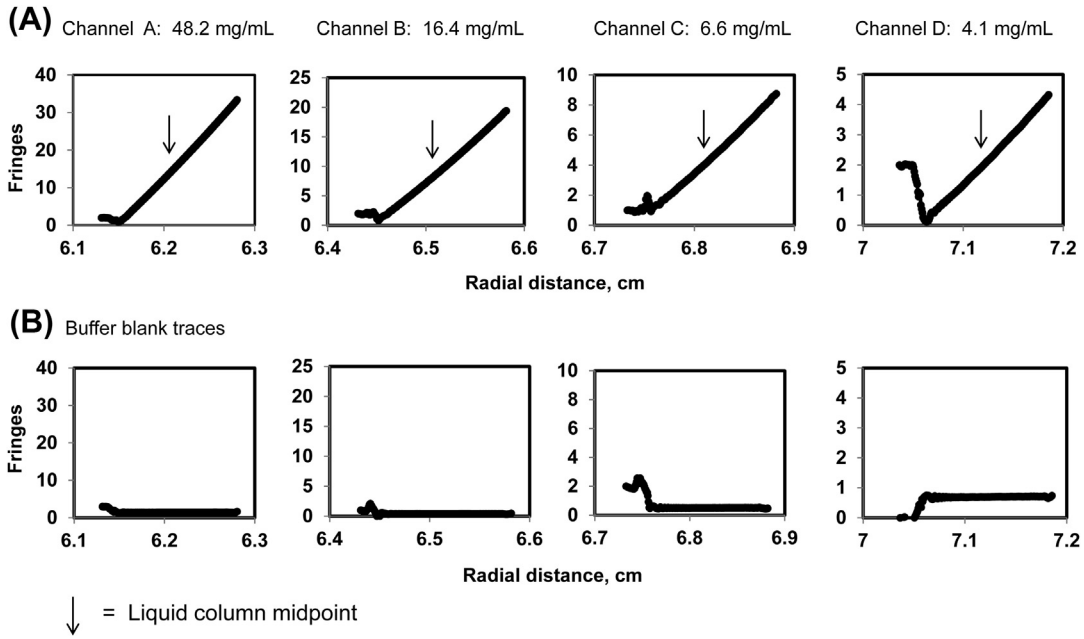

FIGURE 9.8 Very short column SE-AUC experiments using refractometric detection with the Rayleigh interferometer at 4,000 rpm, 20 °C, using an 8-channel centerpiece, see Figure 9.2(G): (A) on a 150 kDa protein over a range of high protein concentrations in each of the four channels or (B) buffer vs buffer run in all four channels (buffer blank run). All samples reached equilibrium within a few hours. Given the very low centrifugation speed and very short column height, resulting interference plots for buffer vs buffer experiments were all flat with negligible slope. As a result, the need for a buffer blank correction to the corresponding high protein sample experiments was not considered significant given the relative very large and fairly linear refractometric plots recorded for the protein samples. Hence simple assessment of the protein sample's slope at the liquid column height midpoint of the refractometric SE-AUC profile in each channel allowed the apparent M_w for each protein sample to be calculated using Eqn (9.11), in this chapter.

centrifugal field will create a stable density gradient. Under appropriate experimental conditions a density gradient can be generated within the AUC cell between the solution column meniscus and the cell base that spans a solution density that actually includes the buoyant density of the macromolecule of interest in the buffer solution being used. In this situation the macromolecule will form a stable sharp band centered at the radial position in the density gradient where the solution density actually equals the sample molecule's buoyant density (the molecule is neutrally buoyant, which corresponds to when $\overline{v}_2\rho_0 = 1$, see Eqn (9.4)). This method can provide very high resolution in discriminating differences in the buoyant density of macromolecules due to differences in chemical composition.

Such a method has found use in the area of gene therapy where it was used to characterize the structural heterogeneity of the drug delivery system, adenovirus, in terms of their DNA homogeneity content [94,95]. This density-gradient SE-AUC technique was also the AUC method actually used by Meselson & Stahl in their famous DNA replication experiment mentioned at the beginning of this chapter [11]. In general this mode of AUC finds its greatest

use in the preparative purification of very large biology macromolecules e.g., viruses, VLPs, and DNA. However, with the return of interest in the gene therapy area and the development of novel nanoparticle drug delivery systems [94,95] density-gradient SE-AUC in the analytical centrifuge could find significant use in these niche areas of biopharmaceutical development.

It should be noted that implementing density-gradient SE-AUC typically does require some method development to get the density gradient to include the actual buoyant density of the species in the sample and to find a gradient and centrifugal force which together provide appropriate resolution. Such optimization typically includes varying the starting salt conditions and the rotor speed.

9.9 AUC DETECTORS

Detectors available on the Beckman–Coulter analytical ultracentrifuge to monitor the migration of proteins during centrifugation consist of a variable wavelength UV–VIS detector for the XL-A and the same UV–VIS detector plus a Rayleigh interferometer (a differential refractometer) for the XL-I. In addition to these two detectors a fluorescence detector made as a third-party add-on detector for the Beckman–Coulter XL-A or XL-I centrifuge can be obtained from AVIV Biomedical, Inc. Details concerning the use of these detectors can be found in references by Demeler [66] and Laue [96,97]. The following sub-sections provide some brief highlight points concerning each of these detectors.

9.9.1 Variable Wavelength UV–VIS Detector

By far the most commonly used detector in AUC work in the biopharmaceutical industry is the UV detector. Its overall simplicity in terms of sample preparation, its specificity in detecting only UV-absorbing material, and its ability to potentially differentiate between materials in terms of their absorptivity profiles make it the detector of choice. However, the analyst should keep in mind the following points when using this detector:

1. Due to the mechanical movement of the slit assembly across the photomultiplier tube to record a complete single data scan (in velocity scan mode) of an AUC requires about 1 minute from start to finish. This relatively slow scan speed limits the number of scans that can be acquired, especially when using the 8-hole rotor, which in turn impacts the extent of signal averaging which is possible, and which might influence the maximum rotor speed that can be used. Further, although this scan time is small relative to the timescale associated with the migration of macromolecules during an AUC experiment, the fact that the boundary moves slight from the beginning to the end of each scan could have some impact on AUC experiments being analyzed using today's modern high resolution and precision analysis software if not accounted for (Note: Recent improvements in SEDFIT actually take this effect into account during data analysis [98,99]). Scan rate is not an issue for sedimentation equilibrium experiments and such scans generally use finer radial point spacing and averaging of ~20 measurements at each radial position to improve the signal/noise ratio, which means scanning each cell in equilibrium mode may take 20-30 minutes.

2. Attempts to use different wavelengths to allow different concentrations of samples to be run in a single AUC run are limited due to the fact that the monochromator does not accurately return to its exact set wavelength, causing slight differences in the actual OD from scan to scan. Such scan-to-scan scaling shifts pose major problems for most approaches to analyzing sedimentation velocity data (the vH-W method is an exception). Variability of the measurement wavelength is less of a problem for sedimentation equilibrium data analysis (it simply leads to a slight extra uncertainty in the association constants) and hence multiple wavelengths are commonly used with sedimentation equilibrium protocols to expand the concentration range that can be covered.
3. Acquiring the UV-VIS scans in intensity mode (separately recording the light intensities for the sample and reference channels) rather than absorbance mode may offer a reduction in the signal noise by a factor of $(2)^{0.5} = 1.414$ [66]. However doing this gives up one important advantage that UV-VIS scans have over RI scans: absorbance scans have a true zero reference (zero absorbance has a unique physical meaning). Analyzing the UV-VIS intensity data requires treating the zero reference for each scan as an adjustable fitting parameter, thus introducing dozens to hundreds of extra fitting parameters. Tests in the authors' laboratories indicate that this can lead to less reliable detection and quantitation of minor peaks. when using $c(s)$ analysis.
4. Attention needs to be paid to the intensity of the xenon lamp output (which is strongest in the UV part of the spectrum, with a maximum output at 230 nm) due to accumulation of UV-absorbing deposits on the lamp enclosure or the window cover over the lamp. Some instruments lack the extra window which can easily be removed for cleaning; if such a cover is not used the lamp will need to be cleaned every few runs to maintain good S/N.
5. The signal to noise ratio with this detector is at best about 100-200:1, which corresponds to an uncertainty (standard deviation) for a 1 OD sample reading of about ± 0.01 to ± 0.005 OD. However it should be noted that actual S/N will depend on the level of transmitted light, which is affected by both the transparency of the sample buffer and the xenon lamp output (which depends on wavelength and the cleanliness of all the optical surfaces).
6. Steep refractive index gradients created during sedimentation boundary runs conducted at high protein concentrations (caused by the actual migration of the protein drug sample) can distort the absorbance readings under appropriate conditions and may actually bend the light beam so much the signal is not seen by the photomultiplier tube. As a result, simply changing the wavelength of the UV detector to higher wavelengths to keep the OD within the normal working range of about 1 OD will not allow the concentration to be increased indefinitely. Factors that influence the highest concentration that can be used without encountering significant distortions include the molecular weight of material being analyzed, rotor speed, and the optical path length of the centerpiece. In general for SV-AUC experiments on a 150 kDa protein at 40K rpm using a 3 mm centerpiece the upper limit is around 20 mg/mL.
7. It is important to keep in mind the linearity of the UV-VIS detector is limited. Many users do not realize that the linearity is significantly different for scans acquired in velocity mode *vs.* equilibrium mode. In velocity mode linearity is compromised in order to speed up the data acquisition. Note that simulations have shown that detector non-linearity can lead to false minor peaks in $c(s)$ analysis [J. S. Philo, unpublished]. Consequently it is recommended to keep the OD at 1 or less during boundary velocity experiments. The

linearity is higher for scans acquired in sedimentation equilibrium mode so the data may be usable up to ~1.5 OD (but this should be tested by the user under the actual experimental conditions).

8. Even when only a single wavelength is being used in a run, the wavelength can sometimes shift or drift slightly (and the likelihood of encountering this will increase with the length of the run). This is particularly a problem when the wavelength chosen is in a region where the sample absorbance increases or decreases steeply with wavelength (which is almost always true when using 230 nm to take advantage of the high light output at that wavelength). Thus when possible it is advantageous to choose a wavelength at an absorbance maximum or minimum. Note that simulations have shown that a wavelength shift or drift during a boundary velocity experiment can produce false peaks from $c(s)$ anal analysis [J.S. Philo, unpublished].

9.9.2 Refractometric Detection Using the Rayleigh Interferometer

The Rayleigh interferometer is effectively a specialized differential refractive index detector whose output measures the difference in refractive index between the protein sample and a reference buffer, which should have exactly the same composition as the buffer in which the protein sample is dissolved. In the previous sentence the words "exactly the same composition" are of key importance because this detector is extremely sensitive in measuring differences in refractive index between two (differences in refractive index as small as 10^{-7} can be detected). Even when using great care it will generally be impossible to make two nominally identical buffer solutions that will match in refractive index to better than 10^{-3}. Since typical working protein concentrations fall into the range of 0.1 to about 50 mg/mL, these solutions will yield corresponding working differential refractive index signals in the range of 10^{-7} to 10^{-5}. Given the magnitudes of these signals, it is easy to see that even a small difference in buffer composition (excipient concentrations) between the reference and the sample can produce a signal (a zero offset) that is orders of magnitude larger than the signals arising due to sedimentation of the macromolecule. If the buffer components did not sediment at all this would simply produce a constant signal (an offset) that would not be a problem. However at the high rotor speeds used for sedimentation velocity even small molecules like salts sediment to some extent, and higher MW excipients such as sugars, polyols, and detergents can form substantial gradients. Thus any miss-match between the buffer used for the reference sample and that in the actual protein sample can potentially generate large signals.

It therefore becomes an imperative to match the sample solution buffer matrix with the corresponding reference buffer solution as closely as possible. Usually the best way to achieve this is dialysis of the sample solution against the reference buffer solution, and using the final dialysis buffer as the reference. Alternate approaches for buffer matching are repetitive buffer exchange using centrifugal spin concentration cartridges with appropriate membrane molecular weight cutoffs, or using SEC desalting columns. However in the former case one needs to realize the potential impact of generating local very high protein concentrations in the region of the membrane that could induce aggregation, while in the latter case the protein solution will be significantly diluted requiring further concentrating (most likely involving the use of centrifuge spin cartridge!). The effects of such sample handling

(including dialysis) must thus be carefully considered in term of their impact on the samples being studied. The most common use of AUC in the biotech industry is to monitor aggregates, but there is no way to be sure that dialysis or alternate approaches to buffer matching do not alter the aggregate content. This then is the primary reason absorbance detection is used much more widely in the biotech industry than RI detection.

Once the buffer matrix between the protein and reference solution are matched, the investigator is unfortunately faced with a second requirement. Even if the buffers are perfectly matched the signals arising from sedimentation of the buffer components will not perfectly cancel unless the meniscus positions in the sample and reference sectors are exactly the same (unless sedimentation starts from the same radial position). Therefore a second requirement for optimal experiments is matching the solution column heights in the reference and sample compartments of the centrifuge cell. In principle this could potentially could be done by filling both sectors with the exactly the same solution volumes. However, in practice this cannot be done with sufficient accuracy even using manual or automated pipettors. Hence to achieve matching of the reference and sample meniscii one can use either a synthetic boundary centerpiece or a special "meniscus matching centerpiece" originally developed by Walter Stafford, see Figure 9.2(C & D). In using either of these centerpieces the reference sector is filled with 10-20 μL more volume of formulation solution then the volume of sample that is added to the sample sector. The filled and assembled cell is then appropriately placed into the rotor and taken to 8,000 to 10,000 rpm for a short time to force the excess formulation solution to be pushed into the sample sector to achieve the radial matching of both meniscii. Then the rotor is stopped, the cell is removed, and the contents of the sample sector is mixed by repeatedly turning the cells upside down to take advantage of the air bubbles within both sectors of the AUC cell to aid in the mixing process. The cell is then replaced back into the rotor to conduct the normal SV-AUC run on the sample that has now been slightly diluted by 3-5%. It should also be noted that in situations where meniscus mismatch does exist, the program SEDFIT does have capability to deal with meniscus mismatch via software instead of using the hardware approach just outlined here. At present however, it appears that achieving true meniscus matching is preferable, but using software as a fall-back approach might be adequate [100].

Due to the above issues associated with properly preparing a protein drug sample for AUC analysis using the Rayleigh interferometer, this detector has been seldom used in the biopharmaceutical industry. One notable exception is however samples where UV-VIS detection is not an option due to the presence of excipients with strong UV absorption, such as benzyl alcohol or other anti-microbial agents used in multi-dose vials. However, in some situations, especially at very low speeds as discussed in reference [94] and in Section 9.7.2 of this chapter, the normal sample processing required in making AUC runs can be avoided making the use of this detector as easy as that of UV-VIS detection.

One further reason the RI detector is not commonly used in the biotech industry is that the noise in the RI scans is decidedly not random and can be correlated over substantial regions of the cell and over multiple scans. Many industry labs have realized that consequently analyzing RI scans with the $c(s)$ method from samples which should produce no signals (running water or buffer in both the sample and reference channels) will nearly always produce false peaks. Although the area of such false peaks is small (typically hundredths of a

fringe), for proteins samples at 1 mg/mL or less those false peaks can represent minor components at levels of a few tenths of percent. Thus the RI detector can intrinsically produce false peaks at levels that are comparable to minor aggregate species that we would like to detect (and which regulatory agencies say must be characterized). Uncertainty about whether data from the RI detector is reliable enough for detection of minor components in pharmaceuticals is perhaps the most important reason it is seldom used in the industry.

Finally, it should be noted as is common with all differential refractive index detectors, the Rayleigh interferometer has the unique property of being capable of detecting virtually any material as long as its refractive index differs from the refractive index of the solution matrix it is dissolved in. As a result these detectors have been referred to as universal detectors. Hence this property of Rayleigh interferometer makes them very useful in detecting macromolecules that have no or very-weak light-absorbing properties. This property could be put to good use in characterizing very complex protein drugs that are extensively modified with chemical groups that have no useful absorbance bands, e.g. carbohydrates and PEG, by measuring the heterogeneity of the ratio of protein to chemical group adduct by combining RI detection with UV-VIS detection.

9.9.2.1 Use of the Rayleigh Interferometer to Experimentally Assess the Extinction Coefficient of Protein Biopharmaceuticals

An interesting novel use of the Rayleigh interferometer on the XL-I centrifuge in the biopharmaceutical industry is its ability to provide an orthogonal experimental approach (along with an SEC experimental approach discussed in Chapter 7 of this book) for assessing the extinction coefficient of protein biopharmaceuticals [101–103]. This capability to confirm the extinction coefficient value determined by a simple theoretical calculation based on amino acid composition (usually determined from the amino acid sequence) with an actual experimental value, and also to provide an easy way to demonstrate the high similarity of a biosimilar's extinction coefficient to the innovator's extinction coefficient, we believe merits mentioning.

The key to this approach takes advantage of the unique property of proteins that concerns the fact that the change in refractive index per unit weight protein, which is described by a parameter called the refractive index increment ($\partial n/\partial c$), is fairly constant from one protein to another (assuming the protein does not have an extremely unusual amino acid composition that is highly enriched in only a few types of amino acids). This average protein refractive index increment under constant chemical potential and for the wavelength of the Rayleigh interferometer laser in the analytical ultracentrifuge, $(\partial n/\partial c)_{\lambda,\mu}$, has been reported to have a value of 0.183 ml/gm [94]. Given this fact a simple AUC experiment can be conducted using a special centerpiece called a synthetic boundary cell, see Figure 9.2(C), which enables a buffer solution in the reference sector to be layered over a sample solution. In so doing a boundary is created that runs from zero concentration to the concentration of the sample placed in the sample sector. By using the Rayleigh interferometer we can measure the concentration of the sample in terms of change in refractive index and convert it to total concentration (as we well see using Eqn 9.13 below). To carry out this measurement a protein drug sample (at a concentration in the range of a few mg/mL) is first appropriately dialyzed against its formulation buffer. The final dialysis buffer is then

used to appropriately fill the reference sector of the assembled AUC cell containing a synthetic boundary centerpiece with 0.40 mL of buffer. Next an appropriate volume (0.15 mL) of the dialyzed protein drug is placed in the sample sector of the synthetic boundary cell. The filled AUC cell is then placed in the rotor and thermally equilibrated as normal. These cells were then centrifuged at a relatively low speed to layer the reference buffer solution over the dialyzed protein drug samples. On achieving this overlay the resulting interference pattern yields a classical symmetrical boundary with a relatively flat reference region above the protein sample and a relatively flat plateau region after the formed boundary (the resulting pattern would look like what one would obtain in an SV-AUC on a 100% pure protein sample after it had effectively migrated to about the midpoint in the AUC cell). Once this data is collected the run is stopped and the rotor is removed, and the content of each cell is mixed by taking advantage of the large air bubble in each sector of the cell by rocking the rotor or by removing each cell and rocking it. Once the content of each cell's sector is uniformly mixed the cell is appropriately repositioned back into the rotor if it was removed and the rotor is placed back into the centrifuge chamber for thermal re-equilibration. The rotor is taken up to the same speed as was used to record the protein synthetic boundary and refractometric data scans are recorded to use for baseline correction of the previously-recorded synthetic boundary data. Samples of the same dialyzed protein solution that were used to fill the AUC cells were also used to assess their OD at 280 nm on the undiluted samples using 1-mm path length UV cuvettes or accurately diluted with final dialysis buffer so their absorbance could be measured using a 1-cm path length UV cuvettes. Alternatively, it should be noted that it is also possible to measure the absorbance of the same sample used in the AUC experiment to measure total concentration by using the UV detector on the analytical centrifuge [102]. However, some difference can be expected between the absorbance recorded via the analytical centrifuge's UV detector and that measured by a static bench-top spectrophotometer due to the fact that the bandwidth of the UV detector in the centrifuge is likely significantly larger, and also due to its likely lower linearity. Thus some correction or calibration of the OD values observed in the centrifuge may be needed. In additional, in using this approach to obtain the sample's absorbance the question will arise as to what wavelength to use. Given the sample's concentration of a few mg/mL the wavelength will need to be sufficiently removed from the typical protein peak maximum at about 280 nm wavelength. This will then require the measured absorbance in the analytical ultracentrifuge to be scaled appropriately based on the UV spectrum of the sample to obtain the extinction coefficient at 280 nm.

From the recorded data the change in the number of fringes, Δj, was determined for each sample and converted to total sample concentration, mg/mL, using Eqn (9.13) where L corresponds to the pathlength or height of the synthetic boundary centerpiece (1.2 cm) and λ is the wavelength of the laser:

$$\text{Sample concentration}\ (\text{mg/mL}) = \Delta j\left[\lambda/(\partial n/\partial c)_{\lambda,\mu}\right]\text{L} \tag{9.13}$$

The extinction coefficient (at 280 nm) measured from each cell was then obtained by simply dividing the total OD_{280nm} by the total mass concentration of the sample. In cases where the protein is in fact a glycoprotein the actual extinction coefficient obtained will be that for

the total mass. To obtain just the protein extinction coefficient of the drug the $(\partial n/\partial c)_{\lambda,\mu}$ values in Eqn (9.13) will need to be corrected using Eqn (9.14), where an average of 0.14 mL/mg [104] is used for $[(\partial n/\partial c)_{\lambda,\mu}]_{\text{carbohydrate}}$:

$$(\partial n/\partial c)_{\lambda,\mu} = \left[(\partial n/\partial c)_{\lambda,\mu}\right]_{\text{protein}} (\%\ \text{protein}) + \left[(\partial n/\partial c)_{\lambda,\mu}\right]_{\text{carbohydrate}} (\%\ \text{carbohydrate}) \tag{9.14}$$

Using this new value for $(\partial n/\partial c)_{\lambda,\mu}$ the resulting sample concentration needs to be now multiplied by the % protein. This value for the total protein concentration is then divided into the total sample OD_{280nm} to obtain the protein extinction coefficient for that sample.

If a solution of some appropriate protein standard can be prepared at an accurately known weight concentration (perhaps another protein drug product whose extinction coefficient is accurately known) an alternate approach can be used that does not require explicitly assigning a value to the refractive increment. In this case the ratio of the total fringe displacements, Δj, for the unknown sample to that for the standard directly gives the ratio of the two concentrations. (But this still implicitly assumes the refractive increments are the same for the two proteins).

It should be noted that this same information could be obtained during a normal SV-AUC experiment assuming any refractive index change from the mismatch in the meniscus for the protein sample and reference dialysis buffer could be appropriately accounted for [100] and no material was lost to the base of the centrifuge cell before the first data scan was taken. Hence agreement between both values, within experimental uncertainty, would support the absence of any significant amount of very low and/or high MW material (especially non-UV-absorbing contaminants) in the sample.

9.9.2.2 Difference SV-AUC Using the Rayleigh Interferometer: Increasing the Ability to Assess Changes in the HOS of Protein Biopharmaceuticals

As mentioned earlier in this chapter, one of the key attributes of AUC analysis in the biopharmaceutical industry is its capability for assessing the HOS comparability of protein biopharmaceuticals via the measurement of their monomer sedimentation coefficient. It turns out that this capability can be significantly enhanced by using a technique called difference SV-AUC [39]. In this mode two different samples at the same concentration are compared head to head in a normal double sector centerpiece. In carrying out this measurement one sample is placed in the reference sector while the other sample is placed as usual in the sample sector of the same centerpiece. In loading both sectors the ideal situation is to fill both sectors with exactly the same protein concentration, and also exactly the same volume of solution so that the radial distance of both menisci are the same. However it should be pointed out that the requirement of matching the radial position for both menisci is not mandatory and mismatches in menisci can be accommodated to some extent. In addition a mismatch in initial sample concentration between both samples can also be tolerated if the sample material being investigated displays a sedimentation coefficient that is independent of concentration [39]. Nevertheless, both types of mismatches should be kept as small as possible.

Although this technique can in principle be carried out using either UV−VIS detection or refractometric detection, using the Rayleigh interferometry offers a number of advantages.

These advantages of the Rayleigh interferometer over UV–VIS detection are (1) its higher S/N at the concentrations normally used in these experiments, (2) its superior ability to tolerate steep refractive index gradients without encountering signal distortion, and (3) its ability to generate a greater difference signal in proportion with the higher protein concentrations. With respect to this last point, since for UV-VIS detection the use of high protein concentration requires changing the wavelength to keep the OD in the linear region, the resulting increase in difference signal with concentration is lost. Published work using this technique in the 1970's indicated that it is capable of measuring differences in sedimentation coefficient of 0.01 S for proteins with MWs 30–300 kDa with an uncertainty of ±0.0005 S [39] making it a highly sensitive method for detecting changes in HOS.

It should be noted, however, that the ability to reach this high level of sensitivity did require a significant effort to assure proper alignment of the reference mask, which was a key contributing source of error in these measurements. It may be possible that less than optimal alignments could be tolerated via a correction factor developed using the same sample in both sectors as outlined by Richards and Schachman [105] without incurring too large of a reduction in sensitivity and precision. Unfortunately to our knowledge difference sedimentation experiments with this sensitivity and precision have never been made in the modern era with an XL-I. In addition, to our knowledge none of the current data analysis software packages incorporate routines to evaluate such data. Nevertheless, investigations into this methodology are warranted for evaluating what improvement might be achieved to improve the capability of AUC to detect small differences in conformation.

9.9.3 Fluorescence Detection Using the AU-FDS

Fluorescence detection offered by the AVIV AU-FDS [106] (made by AVIV Biomedical Inc., in Lakewood, NJ) provides the unique capability for studying reversible binding interactions of very high affinity. This is achieved by allowing sample concentrations to be reduced by several orders of magnitude [107]. In addition, this detector system also provides the possibility to study the biophysical solution behavior of protein drugs in complex biological fluids, such as blood plasma [108,109] and at very-high drug concentrations (by spiking these samples with small amounts of fluorescently labeled protein drug as a tracer). However, in all these applications fluorescently-labeled protein molecules are required since intrinsic fluorescence is presently not possible with this detector (which has a fixed excitation wavelength). As a result a significant amount of work is needed to confirm that the fluorescent label placed onto the protein drug does not introduce any artifacts.

9.10 MISCELLANEOUS HELPFUL INFORMATION ABOUT CONDUCTING AUC EXPERIMENTS

- A common misunderstanding for new users of AUC is that the velocity centerpieces made from Epon epoxy resin cannot be used at speeds above 42,000 rpm. While that is indeed the official maximum speed for which Beckman–Coulter guarantees their

performance, most AUC labs routinely use them at speeds up to 60,000 rpm, with the understanding that this will lead to a shorter lifetime and that they cannot expect replacement when the centerpiece fails. That is, most AUC labs in the biotech industry consider the finite lifetime of these centerpieces as a normal operating cost (and a fairly trivial one compared to the investment in the equipment and operator training). Note that when significant leakage occurs at high speed and the fluid level in the two sectors becomes significantly different, the imbalance in fluid pressure will bend (or even break) the center rib between the sectors. Such bending is generally not reversible, so the centerpiece should be discarded even if no damage or distortion can be visibly detected.

- A closely-related issue is why don't biotech AUC labs use the aluminum centerpieces, which are rated to 60,000 rpm by Beckman—Coulter, instead of the charcoal-Epon ones? The main problem with the aluminum centerpieces is that some protein samples will aggregate irreversibly in these cells, despite the fact that the centerpiece surfaces have been converted to aluminum oxide to try to make them more biocompatible. Similarly AUC users in the biotech industry generally avoid the aluminum-filled versions of the Epon centerpieces in favor of the charcoal-filled versions to avoid any possible sample exposure to aluminum.[2] Titanium centerpieces are also available from Nanolytics in Germany, but to our knowledge the relative inertness of those centerpieces relative to charcoal-filled Epon has not been extensively evaluated. Note too that the extra weight of a titanium centerpiece requires also purchasing a special titanium version of the counterweight.
- Hex head filling screws, in combination with an appropriate torque screw driver, provided by Spin Analytical Inc. represent an excellent improvement over the simple flat-head filling screws provided by Beckman—Coulter. This improvement avoids the common outcome of stripping these brass screws, but more importantly provides a very reliable route for sealing the cells without distorting the cell housing by overtightening these screws. Such overtightening can make the insertion of the assembled cell into the centrifuge rotor very difficult. Overall, what might at first appear to be a minor contribution, we feel merits significant applause.
- The development of centerpieces with path lengths significantly smaller than the 3-mm 2-channel centerpieces made by Beckman—Coulter would be of significant help in allowing the application of AUC to higher protein drug concentrations. At this time the thinnest centerpieces that can be obtained commercially are the titanium 1.5-mm centerpieces made by Nanolytics [110].
- Although the XL-A and XL-I analytical ultracentrifuges are stated to be capable of running at temperatures up to 40 °C, it turns out the deposition of diffusion pump oil on the optical elements within the chamber effectively prohibits the running of centrifuge at temperatures much above 30 °C. However, the commercial introduction of a turbomolecular pump (which is now a standard equipment on Beckman-Coulter

[2]Although during manufacturing of the aluminum-filled Epon centerpieces the aluminum particles exposed at the surface are removed via a chemical treatment, it is unclear whether additional aluminum exposure occurs as a consequence of mechanical stress during repeated use. Note also that although the aluminum-filled versions were created in an attempt to improve the thermal conductivity of the centerpieces, in reality there is no significant improvement over the charcoal-filled versions.

analytical ultracentrifuges) allows the analytical ultracentrifuge to now be capable of running at its stated maximum operation temperature specification. Turbomolecular pumps can be retrofitted on older instruments having diffusion pumps. This innovation is due to the efforts of Walter Stafford (at BBRI) and Rich Cole (at Beckman—Coulter) and again deserves applause.

- In general it is generally a good idea to keep all components common to a given AUC cell together, to assemble them in the exact same way in terms of orientation, and to always use that cell in the same position (hole number) in the rotor. This practice can be very helpful in developing historical information for use in detecting when AUC cells or cell components are displaying performance problems and may need to be replaced.
- Although the XL-I is stated to be capable of running both the UV—VIS and RI detectors in the same run over its entire range of rotor speeds, problems may be encountered when at speeds above approximately 45,000 rpm. These problems are related to overloading the data acquisition processor in the instrument, so they are aggravated when running larger numbers of cells in the run. Note too that the noise level of the RI detector also typically increases at speeds above ~50,000 rpm.
- For samples at relatively low concentrations it is helpful to improve the S/N ratio of the RI detector by using special cell window holders incorporating so-called "interference slits." These narrow masks ensure that the laser beams hit exactly the same narrow regions of the cell windows with every light pulse, independent of any pulse timing variability. The improvement in S/N is noticeable, but usually not dramatic; it will vary from one instrument to another, and is generally most significant at higher rotor speeds (where the improvement may be approximately two- to threefold). Unfortunately these narrow slits are not compatible with acquiring absorbance scans for that cell. These special window holders are available through Spin Analytical.

9.11 CONCLUSION

The analytical ultracentrifuge is a powerful biophysical tool that can help assist the biopharmaceutical scientist in assessing a protein drug's total level of aggregation, characterize its heterogeneity and the consistency of the HOS of its monomeric form (via measurements of its sedimentation coefficient), and measure its biophysical properties in solution (e.g., detection of reversible self-association). Such information is of great importance, making AUC an indispensable tool in developing biopharmaceuticals.

In writing this chapter we were well aware that a large number of reviews of AUC and its capabilities already exist. As a result we have focused our efforts in this particular review on the specific needs of today's working biopharmaceutical scientists, as well as those just starting out in this field or planning to enter the biopharmaceutical industry. In so doing we have taken a closer look at how the analytical ultracentrifuge can be, and is being, used in the biotechnology industry. This has also led us to revisit some of the older, much less commonly employed, modes of AUC analysis that many of today's biopharmaceutical scientists are most likely not familiar with, which we feel may prove to be of value to them. In discussing these seldom-used modes of AUC analysis we have also tried to point to specific areas where these capabilities could be useful. At the same time we have also highlighted some areas

where improvements are needed or where opportunities exist that could make the analytical ultracentrifuge an even more important and effective contributor to the development process of protein biopharmaceuticals.

However, like all good instruments the analytical ultracentrifuge needs the attention of its manufacturer, as well as its end-users, to reach its full potential by making sure its hardware and data acquisition software operates to its full capability and stays current with present day technology. Hence we can only hope that ongoing efforts to improve and expand the hardware capabilities of the current instrument [33,35,111–113], and to develop a next-generation "open source" AUC instrument [75], the full potential of the analytical ultracentrifuge will be realized to enhance its role in both current and new areas of biopharmaceutical development.

References

[1] Bowen J, Rowe A. An introduction to ultracentrifugation. London: John Wiley & Sons; 1970.
[2] Lewis M, Weiss G. Fifty years of the ultracentrifuge. Oxford: North Holland; 1976.
[3] Svedberg T, Pedersen KO. The ultracentrifuge. Oxford: The Clarendon Press; 1940.
[4] Svedberg T, Rånby BG, Pure I U o, Chemistry A, Division ACPC, Pure I U o, Division ACM. Physical chemistry of colloids and macromolecules. In: Proceedings of the international symposium on physical chemistry of colloids and macromolecules to celebrate the 100th anniversary of the birth of professor The (odor) Svedberg on August 30 1884…. Uppsala University, Sweden, held on August 22–24, 1984. Blackwell Scientific Publications; 1986.
[5] Schachman H. Is there a future for the ultracentrifuge. In: Harding S, Rowe A, Horton J, editors. Analytical ultracentrifugation in biochemistry and polymer science. Redwood Press, Royal Society for Chemistry; 1992. pp. 3–15.
[6] Holde KV, Hansen J. Analytical ultracentrifugation from 1924 to the present: a remarkable history. Chemtracts Biochem Mol Biol 1998;11:933–43.
[7] Righetti PG. Bioanalysis: its past, present, and some future. Electrophoresis 2004;25:2111–27.
[8] Schachman H. Ultracentrifugation in biochemistry. Academic Press; 1959.
[9] Watson J, Crick F. Molecular structure of nucleic acids; a structure for deoxyribose nucleic acid. Nature 1953;171:737–8.
[10] Watson J, Crick F. Genetical implications of the structure of deoxyribonucleic acid. Nature 1953;171:964–7.
[11] Meselson M, Stahl FW. The replication of DNA in *Escherichia coli*. Proc Natl Acad Sci U S A 1958;44:671–82.
[12] Judson HF. The eighth day of creation: the makers of the revolution in biology. Cold Spring Harbor Laboratory Press; 1996.
[13] Giebeler R. The optima XL-A: a new analytical ultracentrifuge with a novel precision absorption optical system. In: Harding S, Rowe A, Horton J, editors. Analytical ultracentrifugation in biochemistry and polymer science. Redwood Press, Royal Society for Chemistry; 1992. pp. 16–25.
[14] Harding S. The analytical ultracentrifuge spins again. Trend Anal Chem 1994;13:439–46.
[15] Harding SE. Analytical ultracentrifugation and the genetic engineering of macromolecules. Biotechnol Genet Eng Rev 1993;11:317–56.
[16] Ralston G. The renaissance of the analytical ultracentrifuge. Today's Life Sci 1991;3.
[17] Schachman HK. Analytical ultracentrifugation reborn. Nature 1989;341:259–60.
[18] Schuster T, Toedt J. New revolutions in the evolution of analytical ultracentrifugation. Curr Opin Struct Biol 1996;6:650–8.
[19] Stafford WF. Sedimentation velocity spins a new weave for an old fabric. Curr Opin Biotechnol 1997;8:14–24.
[20] Cole JL, Hansen JC. Analytical ultracentrifugation as a contemporary biomolecular research tool. J Biomol Tech 1999;10:163–76.
[21] Shire S. Analytical ultracentrifugation and its use in biotechnology. In: Schuster T, Laue T, editors. Modern analytical ultracentrifugation. Boston: Birkhäuser; 1994. pp. 261–97.

[22] Varley PG, Brown AJ, Dawkes HC, Burns NR. A case study and use of sedimentation equilibrium analytical ultracentrifugation as a tool for biopharmaceutical development. Eur Biophys J 1997;25:437–43.
[23] Berkowitz SA. Role of analytical ultracentrifugation in assessing the aggregation of protein biopharmaceuticals. AAPS J 2006;8:E590–605.
[24] Yphantis D, Lary J, Stafford W, Liu S, Olsen P, Hayes D, et al. On line data acquisition for the Rayleigh interference optical system of the analytical ultracentrifuge. In: Schuster T, Laue T, editors. Modern analytical ultracentrifugation. Boston: Birkhäuser; 1994. pp. 209–26.
[25] Laue TM, Austin JB, Rau DA. A light intensity measurement system for the analytical ultracentrifuge. In: Wandrey C, Cölfen H, editors. Analytical ultracentrifugation VIII. Springer Berlin Heidelberg; 2006. pp. 1–8.
[26] Kar SR, Kingsbury JS, Lewis MS, Laue TM, Schuck P. Analysis of transport experiments using pseudo-absorbance data. Anal Biochem 2000;285:135–42.
[27] Van Holde K. Physical biochemistry. 1st ed. Prentice Hall; 1971.
[28] Lewis MS, Junghans RP. Ultracentrifugal analysis of molecular mass of glycoproteins of unknown or ill-defined carbohydrate composition. Methods Enzymol 2000;321:136–49.
[29] Brown PH, Balbo A, Zhao H, Ebel C, Schuck P. Density contrast sedimentation velocity for the determination of protein partial-specific volumes. PloS One 2011;6:e26221.
[30] Casassa EF, Eisenberg H. Thermodynamic analysis of multicomponent solutions. Adv Protein Chem 1964;19:287–395.
[31] Eisenberg H. Biological macromolecules and polyelectrolytes in solution. Oxford: Clarendon Press; 1976.
[32] Krayukhina E, Uchiyama S, Nojima K, Okada Y, Hamaguchi I, Fukui K. Aggregation analysis of pharmaceutical human immunoglobulin preparations using size-exclusion chromatography and analytical ultracentrifugation sedimentation velocity. J Biosci Bioeng 2013;115:104–10.
[33] Arthur KK, Gabrielson JP, Kendrick BS, Stoner MR. Detection of protein aggregates by sedimentation velocity analytical ultracentrifugation (SV-AUC): sources of variability and their relative importance. J Pharm Sci 2009;98:3522–39.
[34] Gabrielson JP, Arthur KK. Measuring low levels of protein aggregation by sedimentation velocity. Methods 2011;54:83–91.
[35] Gabrielson JP, Arthur KK, Stoner MR, Winn BC, Kendrick BS, Razinkov V, et al. Precision of protein aggregation measurements by sedimentation velocity analytical ultracentrifugation in biopharmaceutical applications. Anal Biochem 2010;396:231–41.
[36] Gabrielson JP, Randolph TW, Kendrick BS, Stoner MR. Sedimentation velocity analytical ultracentrifugation and SEDFIT/c(s): limits of quantitation for a monoclonal antibody system. Anal Biochem 2007;361:24–30.
[37] Hughes H, Morgan C, Brunyak E, Barranco K, Cohen E, Edmunds T, et al. A multi-tiered analytical approach for the analysis and quantitation of high-molecular-weight aggregates in a recombinant therapeutic glycoprotein. AAPS J 2009;11:335–41.
[38] Pekar A, Sukumar M. Quantitation of aggregates in therapeutic proteins using sedimentation velocity analytical ultracentrifugation: practical considerations that affect precision and accuracy. Anal Biochem 2007;367:225–37.
[39] Kirschner MW, Schachman HK. Conformational changes in proteins as measured by difference sedimentation studies. I. A technique for measuring small changes in sedimentation coefficient. Biochemistry 1971;10:1900–19.
[40] Schuck P. A model for sedimentation in inhomogeneous media. I. Dynamic density gradients from sedimenting co-solutes. Biophys Chem 2004;108:187–200.
[41] Gabrielson JP, Arthur KK, Kendrick BS, Randolph TW, Stoner MR. Common excipients impair detection of protein aggregates during sedimentation velocity analytical ultracentrifugation. J Pharm Sci 2009; 98:50–62.
[42] Goldberg RJ. Sedimentation in the ultracentrifuge. J Phys Chem 1953;57:194–202.
[43] Balbo A, Schuck P. Analytical ultracentrifugation in the study of protein self-association and heterogeneous protein-protein interactions: protocol for velocity and equilibrium sedimentation. In: Golemis E, Adams P, editors. Protein-protein interactions: a molecular cloning manual. Cold Spring Harbor Laboratory Press; 2006. http://www.ors.od.nih.gov/Pages/home.aspx.
[44] Schuck P. Sedimentation analysis of noninteracting and self-associating solutes using numerical solutions to the Lamm equation. Biophys J 1998;75:1503–12.

[45] Schuck P. On the analysis of protein self-association by sedimentation velocity analytical ultracentrifugation. Anal Biochem 2003;320:104–24.
[46] Schuck P. Sedimentation velocity in the study of reversible multiprotein complexes. In: Schuck P, editor. Protein interactions. US: Springer; 2007. pp. 469–518.
[47] Bridgman WB. Some physical chemical characteristics of glycogen. J Am Chem Soc 1942;64:2349–56.
[48] Schumaker VN, Schachman HK. Ultracentrifugal analysis of dilute solutions. Biochim Biophys Acta 1957;23:628–39.
[49] Stafford WF, 3rd. Boundary analysis in sedimentation transport experiments: a procedure for obtaining sedimentation coefficient distributions using the time derivative of the concentration profile. Anal Biochem 1992;203:295–301.
[50] Stafford WF, 3rd. Boundary analysis in sedimentation velocity experiments. Methods Enzymol 1994;240: 478–501.
[51] Philo JS. Improved methods for fitting sedimentation coefficient distributions derived by time-derivative techniques. Anal Biochem 2006;354:238–46.
[52] http://www.rasmb.org/.
[53] van Holde KE, Weischet WO. Boundary analysis of sedimentation-velocity experiments with monodisperse and paucidisperse solutes. Biopolymers 1978;17:1387–403.
[54] Demeler B, van Holde KE. Sedimentation velocity analysis of highly heterogeneous systems. Anal Biochem 2004;335:279–88.
[55] Demeler B. UltraScan—a comprehensive data analysis software package for analytical ultracentrifugation experiments. In: Scott DJ, Harding SE, Rowe AJ, editors. Analytical ultracentrifugation: techniques and methods. The Royal Society of Chemistry; 2005. pp. 210–30.
[56] Schuck P. Size-distribution analysis of macromolecules by sedimentation velocity ultracentrifugation and Lamm equation modeling. Biophys J 2000;78:1606–19.
[57] Lamm O. Die differentialgleichung der ultazentrifugierung. Ark Mat Astr Fys Part B 1929;21:1–4.
[58] Schuck P, Rossmanith P. Determination of the sedimentation coefficient distribution by least-squares boundary modeling. Biopolymers 2000;54:328–41.
[59] Schuck P, Demeler B. Direct sedimentation analysis of interference optical data in analytical ultracentrifugation. Biophys J 1999;76:2288–96.
[60] Provencher SW. Inverse problems in polymer characterization: direct analysis of polydispersity with photon correlation spectroscopy. Die Makromol Chem 1979;180:201–9.
[61] Provencher SW. CONTIN: a general purpose constrained regularization program for inverting noisy linear algebraic and integral equations. Comput Phys Commun 1982;27:229–42.
[62] Provencher SW. Low-bias macroscopic analysis of polydispersity. Biochem Soc Trans 1991;19:479–80.
[63] Philo JS. Limiting the sedimentation coefficient for sedimentation velocity data analysis: partial boundary modeling and g(s) approaches revisited. Anal Biochem 2011;412:189–202.
[64] Brookes E, Cao W, Demeler B. A two-dimensional spectrum analysis for sedimentation velocity experiments of mixtures with heterogeneity in molecular weight and shape. Eur Biophys J 2010;39:405–14.
[65] Brown PH, Schuck P. Macromolecular size-and-shape distributions by sedimentation velocity analytical ultracentrifugation. Biophys J 2006;90:4651–61.
[66] Demeler B. In: Coligan JE, et al., editors. Methods for the design and analysis of sedimentation velocity and sedimentation equilibrium experiments with proteins, current protocols in protein science; 2010. Chapter 7, Unit 7 13.
[67] Demeler B, Brookes E, Nagel-Steger L. Analysis of heterogeneity in molecular weight and shape by analytical ultracentrifugation using parallel distributed computing. Methods Enzymol 2009;454:87–113.
[68] Arakawa T, Ejima D, Li T, Philo JS. The critical role of mobile phase composition in size exclusion chromatography of protein pharmaceuticals. J Pharm Sci 2010;99:1674–92.
[69] Carpenter JF, Randolph TW, Jiskoot W, Crommelin DJ, Middaugh CR, Winter G. Potential inaccurate quantitation and sizing of protein aggregates by size exclusion chromatography: essential need to use orthogonal methods to assure the quality of therapeutic protein products. J Pharm Sci 2010;99:2200–8.
[70] Philo JS. Is any measurement method optimal for all aggregate sizes and types? AAPS J 2006;8:E564–71.
[71] Philo JS. Comparison of methods for soluble aggregate detection and size characterization, in analysis of aggregates and particles in protein pharmaceuticals. John Wiley & Sons, Inc; 2012. pp. 303–333.

[72] Dam J, Schuck P. Calculating sedimentation coefficient distributions by direct modeling of sedimentation velocity concentration profiles. Methods Enzymol 2004;384:185–212.
[73] Shuck P. Diffusion-deconvoluted sedimentation coefficient distributions for the analysis of interacting and non-interacting protein mixtures. In: Scott DJ, Harding SE, Rowe AJ, editors. Analytical ultracentrifugation: techniques and methods. The Royal Society of Chemistry; 2005. pp. 26–50.
[74] Brown PH, Balbo A, Schuck P. A Bayesian approach for quantifying trace amounts of antibody aggregates by sedimentation velocity analytical ultracentrifugation. AAPS J 2008;10:481–93.
[75] Colfen H, Laue TM, Wohlleben W, Schilling K, Karabudak E, Langhorst BW, et al. The open AUC project. Eur Biophys J 2010;39:347–59.
[76] Vinograd J, Bruner R, Kent R, Weigle J. Band-centrifugation of macromolecules and viruses in self-generating density gradients. Proc Natl Acad Sci U S A 1963;49:902–10.
[77] Fujita H. Foundations of ultracentrifugal analysis. New York: Wiley; 1975.
[78] Lebowitz J, Lewis MS, Schuck P. Modern analytical ultracentrifugation in protein science: a tutorial review. Protein Sci 2002;11:2067–79.
[79] Lebowitz J, Teale M, Schuck PW. Analytical band centrifugation of proteins and protein complexes. Biochem Soc Trans November, 1998;26(4):745–9.
[80] Vinograd J, Bruner R. Band centrifugation of macromolecules in self-generating density gradients. III. Conditions for convection-free band sedimentation. Biopolymers 1966;4:157–70.
[81] Chakrabarti G, Kim S, Gupta Jr ML, Barton JS, Himes RH. Stabilization of tubulin by deuterium oxide. Biochemistry 1999;38:3067–72.
[82] Laue TM. Sedimentation equilibrium as thermodynamic tool. Methods Enzymol 1995;259:427–52.
[83] Philo JS. Analytical ultracentrifugation. In: Jiskoot W, Crommelin DJA, editors. Methods for structural analysis of protein pharmaceuticals. Arlington (VA): AAPS Press; 2005. pp. 379–412.
[84] Attri AK, Minton AP. New methods for measuring macromolecular interactions in solution via static light scattering: basic methodology and application to nonassociating and self-associating proteins. Anal Biochem 2005;337:103–10.
[85] Attri AK, Minton AP. Composition gradient static light scattering: a new technique for rapid detection and quantitative characterization of reversible macromolecular hetero-associations in solution. Anal Biochem 2005;346:132–8.
[86] Fernandez C, Minton AP. Static light scattering from concentrated protein solutions II: experimental test of theory for protein mixtures and weakly self-associating proteins. Biophys J 2009;96:1992–8.
[87] Correia JJ, Yphantis DA. Equilibrium sedimentation in short columns. In: Harding SE, Rowe AJ, Horton JC, editors. Analytical ultracentrifugation in biochemistry and polymer science. Redwood Press, Royal Society for Chemistry; 1992. pp. 231–52.
[88] Laue TM. Short column sedimentation equilibrium analysis for rapid characterization of macromolecules in solution. In: Coulter B, editor. Technical information DS835. Palo Alto, CA, https://www.beckmancoulter.com/wsrportal/bibliography?docname=DS_835.pdf; 1992.
[89] Yphantis DA. Rapid determination of molecular weights of peptides and proteins*. Ann N Y Acad Sci 1960;88:586–601.
[90] Van Holde KE, Baldwin RL. Rapid attainment of sedimentation equilibrium. J Phys Chem 1958;62:734–43.
[91] Chatelier RC, Minton AP. Sedimentation equilibrium in macromolecular solutions of arbitrary concentration. I. Self-associating proteins. Biopolymers 1987;26:507–24.
[92] Hall D, Minton AP. Macromolecular crowding: qualitative and semiquantitative successes, quantitative challenges. Biochim Biophys Acta 2003;1649:127–39.
[93] Lebowitz JL, Helfand E, Praestgaard E. Scaled particle theory of fluid mixtures. J Chem Phys 1965;43:774–9.
[94] Berkowitz SA, Philo JS. Monitoring the homogeneity of adenovirus preparations (a gene therapy delivery system) using analytical ultracentrifugation. Anal Biochem 2007;362:16–37.
[95] Yang X, Agarwala S, Ravindran S, Vellekamp G. Determination of particle heterogeneity and stability of recombinant adenovirus by analytical ultracentrifugation in CsCl gradients. J Pharm Sci 2008;97:746–63.
[96] Laue TM. Choosing which optical system of the optimaTM XL-I analytical ultracentrifuge to use. In: Coulter B, editor. Beckman application note a-1821A. Palo Alto, CA, https://www.beckmancoulter.com/wsrportal/bibliography?docname=1821a(a).pdf; 1996.

[97] Laue TM. Applications of sedimentation velocity ultracentrifugation. In: Jameel. F, Hershenson S, editors. Formulation and process development strategies for manufacturing biopharmaceuticals. Hoboken (NJ): John Wiley & Sons; 2010. pp. 231–51.
[98] Brown PH, Balbo A, Schuck P. On the analysis of sedimentation velocity in the study of protein complexes. Eur Biophys J 2009;38:1079–99.
[99] Zhao H, Brautigam CA, Ghirlando R, Schuck P. In: Coligan JE, et al., editors. Overview of current methods in sedimentation velocity and sedimentation equilibrium analytical ultracentrifugation, current protocols in protein science/editorial board; 2013. Chapter 20, Unit20 12.
[100] Zhao H, Brown PH, Balbo A, Fernandez-Alonso Mdel C, Polishchuck N, Chaudhry C, et al. Accounting for solvent signal offsets in the analysis of interferometric sedimentation velocity data. Macromol Biosci 2010;10:736–45.
[101] Babul J, Stellwagen E. Measurement of protein concentration with interferences optics. Anal Biochem 1969;28:216–21.
[102] Gray R, Stern A, Bewley T, Shire S. Rapid determination of spectrophotometric absorptivity by analytical ultracentrifugation. In: Coulter B, editor. Beckman application note A-1815A. Palo Alto, CA, https://www.beckmancoulter.com/wsrportal/bibliography?docname=a_1815a.pdf; 1995.
[103] Voelker P. Measurement of the extinction coefficient of prostate specific antigen using interference and absorbance optics in the optima XL-A analytical ultracentrifuge. In: Behlke J, editor. Analytical ultracentrifugation; 1995. pp. 162–6. Steinkopff.
[104] Theisen A, Johann C, Deacon MP, Harding SE. Refractive Increment Data-Book for Polymer and Biomolecular Scientists. Nottingham, UK: Nottingham University Press; 2000.
[105] Richards EG, Schachman HK. Ultracentrifuge studies with Rayleigh interference optics.I. General application. J Phys Chem 1959;63:1578–91.
[106] Kingsbury JS, Laue TM. Fluorescence-detected sedimentation in dilute and highly concentrated solutions. Methods Enzymol 2011;492:283–304.
[107] Zhao H, Lomash S, Glasser C, Mayer ML, Schuck P. Analysis of high affinity self-association by fluorescence optical sedimentation velocity analytical ultracentrifugation of labeled proteins: opportunities and limitations. PloS One 2013;8:e83439.
[108] Demeule B, Shire SJ, Liu J. A therapeutic antibody and its antigen form different complexes in serum than in phosphate-buffered saline: a study by analytical ultracentrifugation. Anal Biochem 2009;388:279–87.
[109] Kingsbury JS, Laue TM, Chase SF, Connors LH. Detection of high-molecular-weight amyloid serum protein complexes using biological on-line tracer sedimentation. Anal Biochem 2012;425:151–6.
[110] http://www.nanolytics.de/.
[111] Ghirlando R, Balbo A, Piszczek G, Brown PH, Lewis MS, Brautigam CA, et al. Improving the thermal, radial, and temporal accuracy of the analytical ultracentrifuge through external references. Anal Biochem 2013;440:81–95.
[112] Zhao H, Balbo A, Metger H, Clary R, Ghirlando R, Schuck P. Improved measurement of the rotor temperature in analytical ultracentrifugation. Anal Biochem 2014;451:69–75.
[113] Zhao H, Ghirlando R, Piszczek G, Curth U, Brautigam CA, Schuck P. Recorded scan times can limit the accuracy of sedimentation coefficients in analytical ultracentrifugation. Anal Biochem 2013;437:104–8.
[114] Garcia de la Torre J. Sedimentation Coefficients of complex biological particles. In: Harding S, Rowe A, Horton J, editors. Analytical ultracentrifugation in biochemistry and polymer science. Redwood Press, Royal Society for Chemistry; 1992. pp. 333–45.

Further Reading

[1] Schachman H. Ultracentrifugation in biochemistry. Academic Press; 1959. A classic book on the field of AUC that is well written and even after more than six decades is still relevant to today's problems in the field.
[2] Cantor RC, Schimmel PR. Biophysical chemistry: Part II: techniques for the study of biological structure and function. W.H. Freeman & Company; 1980. This well written chapter on AUC in this book is a very useful starting point to get a quick overview and understanding about the field of AUC and its capabilities.

[3] Scott DJ, Harding SE, Rowe AJ. Analytical ultracentrifugation: techniques and methods. RSC Publishing; 2005. A modern update collection of chapters on AUC concerning key methods and application of AUC to topics of significant interest to the biopharmaceutical scientist.
[4] http://www.analyticalultracentrifugation.com/default.htm and http://www.analyticalultracentrifugation.com/sedphat/default.htm The website home of Peter Schuck's programs SEDFIT and SEDPHAT. These websites are also a great source of information about AUC with references and useful links to other websites.
[5] http://www.ultrascan.uthscsa.edu/. The website home of Borries Demeler's programs ULTRASCAN. Another good website for information about AUC with references and useful links to other websites.
[6] http://www.rasmb.org/. A good website for many key AUC software programs old and new with links to other websites. Also houses and on-line large membership of AUC users who interact on-line.